FLUX DIFFERENCE SPLITTING TECHNIQUES FOR THE EULER EQUATIONS IN NON-CARTESIAN GEOMETRY

P. GLAISTER

NUMERICAL ANALYSIS REPORT 8/85

This work forms part of the research programme of the Institute for Computational Fluid Dynamics at the Universities of Oxford and Reading and was funded by the A.W.R.E., Aldermaston under contract no. NSN/13B/2A88719.

ABSTRACT

The results of two problems, a spherically divergent infinite shock and a converging cylindrical shock, are presented. The method is Roe's flux difference splitting in one dimension, applied to cylindrically and spherically symmetric geometries, with a technique for dealing with source terms. The numerical results compare favourably with those in Noh's recent survey, and also with those of Ben-Artzi and Falcovitz using a more complicated Riemann solver.

1. INTRODUCTION

The (linearised) approximate Riemann solver of Roe [1] has proved to be very successful in its application to one-dimensional problems with slab symmetry governed by the Euler equations, (see Appendix A, [2,3,4]). We here seek to extend this technique to one-dimensional problems with cylindrical and spherical symmetry, and/or with source terms. The resulting method is applied to some strongly shocked flows in cylindrical and spherical geometry. The technique is simpler than alternative methods [5,6] and the results compare favourably.

In §2 we derive in detail differential equations for the flow of an inviscid perfect gas in a general orthogonal curvilinear co-ordinate system for the general equations for fluid flow. This is in order to make clear the origin of the non-cartesian terms in the subsequent equations. In §3 we describe the details of the flux difference splitting scheme for the approximate solution of the equations given in §2 in the case of an ideal gas whose flow can be described by one curvilinear space co-ordinate only. In §4 we discuss the properties of the scheme given in §3 while in §5 we describe two specific test problems that can be used to test such schemes. Finally in §6 we display the numerical results achieved for these two problems and compare them with solutions obtained by existing algorithms.

2. EQUATIONS OF FLOW

In this section we consider the Euler equations for modelling the time dependent flow of an inviscid, compressible fluid that is symmetric with respect to one of the co-ordinates in a general orthogonal curvilinear co-ordinate system (x_1, x_2, x_3).

2.1 We first derive the system of differential equations for a fluid by considering a fixed control volume δV with surface δS and unit outward normal $\underline{n}$ to this surface.

By considering the flow passing through this volume we obtain the following integral form of conservation laws

Conservation of mass
$$\frac{\partial}{\partial t}\int_{\delta V} \rho dV = -\int_{\delta S} \rho \underline{u}\cdot\underline{n}\, dS \qquad (2$$

Conservation of momentum
$$\frac{\partial}{\partial t}\int_{\delta V} \rho \underline{u} dV + \int_{\delta S} \rho \underline{u}(\underline{u}\cdot\underline{n})dS = \int_{\delta S} \underline{\underline{T}}\cdot\underline{n} dS \qquad (2$$

Conservation of energy
$$\frac{\partial}{\partial t}\int_{\delta V} e dV = \int_{\delta S} (\underline{u}\cdot\underline{\underline{T}})\cdot\underline{n} dS + \int_{\delta S} e\underline{u}\cdot\underline{n} dS \qquad (2$$

where $\rho = \rho(\underline{x},t)$, $\underline{u} = \underline{u}(\underline{x},t) = (u_1(\underline{x},t),\ u_2(\underline{x},t),\ u_3(\underline{x},t))$ and $e = e(x,t)$ represent the density, velocity in the three co-ordinate directions and the total energy, respectively, at a general position in space $\underline{x} = (x_1,x_2,x_3)$ and at time t.

We assume that we are dealing with a perfect fluid, in which case the stress tensor is given by

$$\underline{\underline{T}} = -p\,\underline{\underline{I}} \quad ,$$

where $\underline{\underline{I}}$ is the identity matrix, and $p = p(\underline{x},t)$ is the pressure. We note that the total energy is given by

$$e = \rho i + \tfrac{1}{2}\rho \underline{u}\cdot\underline{u} \qquad (2.$$

where $i = i(\underline{x},t)$ is the specific internal energy, and we also assume the equation of state for an ideal gas, namely

$$p = (\gamma - 1)\rho i \qquad (2.$$

where γ is the ratio of the specific heat capacities for the fluid.

We now use the divergence theorem applied to both tensors and vectors to write equations (2.1)-(2.3) together with equations (2.4)-(2.5) in differential form to give the set of conservation laws

$$\rho_t + \text{div}\,(\rho\underline{u}) = 0 \qquad (2.6$$

$$(\rho\underline{u})_t + \text{div}(\rho\underline{u}\,\underline{u} - \underline{\underline{T}}) = \underline{0} \qquad (2.7$$

$$e_t + \text{div}\,(e\underline{u} - \underline{u}\cdot\underline{\underline{T}}) = 0 \qquad (2.8$$

together with

$$e = \frac{p}{\gamma - 1} + \tfrac{1}{2}\rho\underline{u}\cdot\underline{u} \qquad (2.9$$

and

$$\underline{\underline{T}} = -\,p\underline{\underline{I}} \quad . \qquad (2.10$$

In the case of a perfect fluid, $\underline{\underline{T}} = -\,p\underline{\underline{I}}$ and using the result from vector analysis[†] that

$$\text{div}\,(\alpha\underline{\underline{B}}) = \alpha\,\text{div}\,\underline{\underline{B}} + (\text{grad}\,\alpha)\cdot\underline{\underline{I}} \quad ,$$

where α is a scalar, we obtain

$$\text{div}\,\underline{\underline{T}} = \text{div}\,(-p\underline{\underline{I}}) = -\,(\text{grad}\,p)\cdot\underline{\underline{I}} = -\,\text{grad}\,p$$

since $\text{div}\,\underline{\underline{I}} = \underline{0}$. Therefore equations (2.6)-(2.9) become

$$\rho_t + \text{div}\,(\rho\underline{u}) = 0 \qquad (2.11$$

$$(\rho\underline{u})_t + \text{div}\,(\rho\underline{u}\,\underline{u}) = -\,\text{grad}\,p \qquad (2.12$$

$$e_t + \text{div}\,(\underline{u}(e + p)) = 0 \qquad (2.13$$

together with

$$e = \frac{p}{\gamma - 1} + \tfrac{1}{2}\rho\,\underline{u}\cdot\underline{u} \quad . \qquad (2.14$$

We notice the emergence of a 'non-divergence' term in equation (2.12), namely grad p, which arises because the stress tensor is diagonal.

(†) Expressions for div $\underline{b}$, div $\underline{\underline{B}}$ and grad α where $\underline{b}$, $\underline{\underline{B}}$ and α are vectors, tensors and scalars repectively, for a general orthogonal curvilinear co-ordinate system are given in Appendix B.

Now for a general orthogonal curvilinear co-ordinate system grad and div are generally different although they are identical for cartesian geometry. Thus care has to be taken when we are working in a co-ordinate system other than cartesian, e.g. spherical polars, since equations (2.11)-(2.14) do not appear in the standard conservation form for the application of conservative finite difference techniques.

2.2 If we now consider flow that is wholly dependent on one of the co-ordinate directions, say x_1, then equations (2.11)-(2.14) become

$$\rho_t + \frac{1}{h_1 h_2 h_3} \frac{\partial}{\partial x_1} (h_2 h_3 \rho u) = 0 \qquad (2$$

$$(\rho u)_t + \frac{1}{h_1 h_2 h_3} \frac{\partial}{\partial x_1} (h_2 h_3 \rho u^2) = - \frac{1}{h_1} \frac{\partial p}{\partial x_1} \qquad (2$$

$$e_t + \frac{1}{h_1 h_2 h_3} \frac{\partial}{\partial x_1} (h_2 h_3 u(e + p)) = 0 \qquad (2$$

together with

$$e = \frac{p}{\gamma - 1} + \tfrac{1}{2}\rho u^2 \qquad (2$$

where h_1, h_2, h_3 are given as usual by the line element $\underline{ds}$ with

$$\underline{ds} = h_1 \, dx_1 \, \hat{\underline{x}}_1 + h_2 \, dx_2 \, \hat{\underline{x}}_2 + h_3 \, dx_3 \, \hat{\underline{x}}_3 \quad ,$$

($\hat{\underline{x}}_i$ is the unit vector parallel to the co-ordinate lines with x_i increasing), and $\rho = \rho(x_1,t)$, $\underline{u} = (u(x_1,t),0,0)$, $p = p(x_1,t)$ and $e = e(x_1,t)$. Equations (2.15)-(2.18) cannot now, however, be written directly in the standard conservation form

$$\underline{w}_t + (\underline{F}(\underline{w}))_{x_1} = \underline{0} \quad , \qquad (2.$$

with $\underline{w} = (\rho, \rho u, e)^T$ and $\underline{F}$ a suitable vector-valued flux function. They can, however, be put in the form

$$(h_1h_2h_3\rho)_t + (h_2h_3\rho u)_{x_1} = 0 \qquad (2.2$$

$$(h_1h_2h_3\rho u)_t + (h_2h_3\rho u^2)_{x_1} = - h_2h_3 \frac{\partial p}{\partial x_1} \qquad (2.2$$

$$(h_1h_2h_3\, e)_t + (h_2h_3u(e + p))_{x_1} = 0 \qquad (2.2$$

Thus in the case $h_1 = 1$, these equations can be written

$$(h_1h_2h_3\rho)_t + (h_1h_2h_3\rho u)_{x_1} = 0 \qquad (2.2$$

$$(h_1h_2h_3\rho u)_t + (h_1h_2h_3(p + \rho u^2))_{x_1} = p \frac{\partial}{\partial x_1}(h_1h_2h_3) \qquad (2.2$$

$$(h_1h_2h_3e)_t + (h_1h_2h_3u(e + p))_{x_1} = 0 \qquad (2.2$$

and it is these equations we now study together with

$$e = \frac{p}{\gamma - 1} + \tfrac{1}{2}\rho u^2 \quad . \qquad (2.2$$

Equations (2.23)-(2.26) are nearer to a "conservation" like form but with an additional "source" like term on the right hand side.

Now in a general orthogonal curvilinear co-ordinate system $dV = h_1h_2h_3\, dx_1\, dx_2\, dx_3$, and thus equations (2.20)-(2.22) could also have been derived from the integral form given by equations (2.1)-(2.3) where a quantity such as $h_1h_2h_3\,\rho\, dx_1\, dx_2\, dx_3$ represents the mass in a control volume bounded by surfaces h_1 = constant, h_2 = constant and h_3 = constant.

2.3 An example of a flow described by the above equations when $h_1 = 1$, and the flow is wholly dependent on x_1 is that of an inviscid, compressible fluid through a duct of smoothly varying cross-section, often referred to as 'duct flow'. In that case we have

$$(S(r)\rho)_t + (S(r)\rho u)_r = 0 \qquad (2.27)$$

$$(S(r)\rho u)_t + (S(r)(p + \rho u^2))_r = pS'(r) \qquad (2.28)$$

$$(S(r)e)_t + (S(r)u(e + p))_r = 0 \qquad (2.29)$$

together with

$$e = \frac{p}{\gamma - 1} + \tfrac{1}{2}\rho u^2 \qquad (2$$

where we write $x_1 = r$ for notational simplicity, and $S(r)$ represents the cross-section of the duct at r. ($S(r) = h,h,h$).

More importantly, equations (2.27)-(2.30) cover all one-dimensional flows including, for example, cylindrical and spherical flows with axial or radial symmetry. They also reduce to the correct form in the much studied case $S \equiv 1$ (slab symmetry).

Equations (2.27)-(2.29) can be written as the system

$$S(r)\underline{w}_t + (S(r)\underline{F}(\underline{w}))_r = \underline{g}(\underline{w}) \qquad (2$$

where

$$\underline{w} = \begin{pmatrix} \rho \\ \rho u \\ e \end{pmatrix}, \quad \underline{F}(\underline{w}) = \begin{pmatrix} \rho u \\ p + \rho u^2 \\ u(e + p) \end{pmatrix} \quad \text{and} \quad \underline{g}(\underline{w}) = \begin{pmatrix} 0 \\ pS'(r) \\ 0 \end{pmatrix} \qquad (2$$

We notice that $S(r)\underline{F}(\underline{w}) = \underline{F}(S(r)\underline{w})$ and $S(r)\underline{w}_t = (S(r)\underline{w})_t$, so that equations (2.31)-(2.32) can be rewritten immediately in the more familiar form

$$\underline{W}_t + (\underline{F}(\underline{W}))_r = \underline{g}(\underline{w}) \ , \qquad (2.$$

where $\underline{W} = S(r)\underline{w}$. This gives rise to new 'conserved' variables R, M, E where $R = S(r)\rho$, $M = S(r)m$ and $E = S(r)e$. (Here m denotes the momentum ρu). It also gives a new 'pressure' variable $P = S(r)p$. (N.B. the velocity $u = U$, sound speed $a = \sqrt{\frac{\gamma p}{\rho}} = \sqrt{\frac{\gamma P}{R}}$ and enthalpy $h = (e + p)/\rho = (E + P)/R = H$ remain the same).

Using these new variables the Euler equations for duct flow become

$$\begin{pmatrix} R \\ RU \\ E \end{pmatrix}_t + \begin{pmatrix} RU \\ P + RU^2 \\ U(E + P) \end{pmatrix}_r = \begin{pmatrix} 0 \\ \frac{S'(r)}{S(r)} P \\ 0 \end{pmatrix} \qquad (2.3$$

with

$$E = \frac{P}{\gamma - 1} + \tfrac{1}{2} RU^2 \qquad (2.$$

Equations (2.34)-(2.35) represent a system of hyperbolic 'conservation' laws similar to equations (2.31) for slab symmetry, i.e. when $S \equiv 1$, $\underline{g} = \underline{0}$, with an additional source term on the right hand side. This additional term is due to the difference between the divergence and gradient operators in a non-cartesian co-ordinate system, in one dimension. Moreover the extra pressure term is due solely to the non-parallel nature of the sides of a control volume in the duct, i.e. on the non-cancelling of pressure terms on either side of the duct.

In the next section we describe a finite difference approximation that models equations (2.34)-(2.35) using the linearised Riemann solver of Roe [1].

3. FLUX DIFFERENCE SPLITTING

In this section we consider a finite difference approximation for the solution of equations (2.34)-(2.35).

3.1 In the case of slab symmetry, $S \equiv 1$, equations (2.34)-(2.35) reduce to the one-dimensional Euler equations in a single cartesian co-ordinate, which can be solved by flux difference splitting using the approximate Riemann solver developed by Roe [1]. Roe's approximate Riemann solver, combined with the 'Superbee' limiter has been used very successfully to give a second order method for the Euler equations in one dimension. (See Appendix A, [2,3,4]). It is found that the first order part of the method captures shocks crisply over a single cell and the second order part gives good accuracy in smooth regions, while the use of a limiter gives sharp contact discontinuities. The scheme is also conservative.

We shall use the similarity of equations (2.34)-(2.35) with the cartesian case to develop a corresponding method for duct flows keeping as far as possible the above valuable properties.

3.2 We consider a fixed grid in space and time with grid sizes $\Delta r, \Delta t$, respectively, and label the points so that $r_j = r_{j-1} + \Delta r$, $t_n = t_{n-1} + \Delta t$ and $\underline{W}_j^n$, $\underline{w}_j^n$ denote the approximation to $\underline{W}(r_j,t_n)$, $\underline{w}(r_j,t_n)$ respectively. (We note here that it is a simple matter to take non-constant time steps Δt_n: it may be useful, for example, to choose Δt_n so as to be able to take the maximum time step consistent with the CFL condition. It is, however, more difficult to generalise to variable space steps Δr_j and preserve accuracy, but it is hoped to deal with this aspect in a later report).

Using the relationship $\underline{W}(r_j,t_n) = S(r_j)\underline{w}(r_j,t_n)$, we may write

$$\underline{W}_j^n = \hat{S}_j \underline{w}_j^n \quad , \tag{3.}$$

where $\hat{S}_j$ represents an average value of $S(r)$. Assuming that at any time $t_n = n\Delta t$ $\underline{W}_j^n$ represents a piecewise constant approximation to $\underline{W}(r_j,t_n)$ in the interval $(r_j - \Delta r/2,\ r_j + \Delta r/2)$ (as in the usual Godunov approach), $\hat{S}_j$ is given by the volume integral[†]

$$\hat{S}_j = \frac{1}{\Delta r} \int_{r_j - \Delta r/2}^{r_j + \Delta r/2} S(r)\,dr \tag{3.}$$

This enables us to project our initial data $\underline{w}(r,0)$ onto a set of piecewise constant states $\underline{W}_j^0$ approximating $\underline{W}(r,0)$, march forward in time, and obtain an approximate solution

$$\underline{w}_j^n = \underline{W}_j^n / \hat{S}_j \tag{3.}$$

for $\underline{w}(r_j,t_n)$ at time $t = t_n$.

Consider the interval $[r_{j-1},r_j]$ and denote by $\underline{W}_L$, $\underline{W}_R$ the approximation to $\underline{W}$ at r_{j-1}, r_j respectively. We now rewrite equations (2.33) as

---

(†) N.B. $\int_{r_j - \Delta r/2}^{r_j + \Delta r/2} S(r)\,dr$ is the volume of an elemental control volume in the duct.

$$\underline{W}_t + \frac{\partial \underline{F}}{\partial \underline{W}} \underline{W}_r = \underline{g}(\underline{w})$$

and solve approximately the associated Riemann problem

$$\underline{W}_t + A\underline{W}_r = \underline{g}(\underline{w}) \qquad (3.4$$

with data $\underline{W}_L, \underline{W}_R$ either side of the point $r_{j-\frac{1}{2}}$, (and linearise by considering A as a constant matrix). We use the approximate form

$$\frac{\underline{W}_P^{n+1} - \underline{W}_P^n}{\Delta t} + \tilde{A} \frac{(\underline{W}_j - \underline{W}_{j-1})}{\Delta r} = \tilde{\underline{g}}(\underline{w}^n) \qquad (3.5$$

where $\tilde{A}$ is the Roe matrix (3.6) given below, $\tilde{\underline{g}}$ is an approximation to $\underline{g}(\underline{w})$ and P may be L or R. The Roe matrix $\tilde{A}$ is an approximation to the Jacobian $A = \frac{\partial \underline{F}}{\partial \underline{W}}$ and is given by

$$\tilde{A} = \begin{pmatrix} 0 & 1 & 0 \\ \frac{(\gamma-3)}{2}\tilde{U}^2 & (3-\gamma)\tilde{U} & \gamma-1 \\ \frac{(\gamma-1)\tilde{U}^3}{2} - \tilde{H}\tilde{U} & \tilde{H} - (\gamma-1)\tilde{U}^2 & \gamma\tilde{U} \end{pmatrix} \qquad (3.6$$

where $\tilde{Y}$ denotes a square root mean of left and right states, namely,

$$\tilde{Y} = \frac{\sqrt{R_L}\, Y_L + \sqrt{R_R}\, Y_R}{\sqrt{R_L} + \sqrt{R_R}} \qquad (3.7)$$

for all variables other than R and ρ, in which case we average

$$\tilde{R} = \sqrt{R_L R_R}, \quad \tilde{\rho} = \sqrt{\rho_L \rho_R} \quad . \qquad (3.8)$$

The eigenvalues of $\tilde{A}$ are

$$\lambda_1 = \tilde{U} + \tilde{a}, \qquad \lambda_2 = \tilde{U} - \tilde{a}, \qquad \lambda_3 = \tilde{U} \qquad (3.9)$$

with corresponding eigenvectors

$$\underline{e}_1 = \begin{pmatrix} 1 \\ \tilde{U} + \tilde{a} \\ \tilde{H} + \tilde{U}\tilde{a} \end{pmatrix}, \quad \underline{e}_2 = \begin{pmatrix} 1 \\ \tilde{U} - \tilde{a} \\ \tilde{H} - \tilde{U}\tilde{a} \end{pmatrix}, \quad \underline{e}_3 = \begin{pmatrix} 1 \\ \tilde{U} \\ \frac{1}{2}\tilde{U}^2 \end{pmatrix} \qquad (3.10)$$

(as in the standard cartesian case when $S \equiv 1$), where $\tilde{H}$ is calculated

using equation (3.7) and the mean sound speed $\tilde{a}$ is calculated from

$$\tilde{a}^2 = (\gamma - 1)(\tilde{H} - \tfrac{1}{2}\tilde{U}^2) \quad . \qquad (3.$$

(N.B. since $|(\underline{e}_1, \underline{e}_2, \underline{e}_3)| = \frac{2\tilde{a}^3}{(\gamma-1)}$, the eigenvectors are linearly independent if and only if $\tilde{a} \neq 0$).

We now use one of the properties[†] of $\tilde{A}$ to write equations (3.5) in the form

$$\frac{\underline{W}_p^{n+1} - \underline{W}_p^n}{\Delta t} + \frac{\underline{F}_j - \underline{F}_{j-1}}{\Delta r} = \tilde{\underline{g}}(\underline{w}^n) \qquad (3.$$

where $\tilde{\underline{g}}(\underline{w}^n)$ is a suitable approximation to the term $\underline{g}(\underline{w})$ on the right hand side of equations (3.4). We thus obtain

$$\underline{W}_p^{n+1} - \underline{W}_p^n = \Delta t\, \tilde{\underline{g}}\,(\underline{w}^n) - \frac{\Delta t}{\Delta r}(\underline{F}_j - \underline{F}_{j-1}) \quad . \qquad (3.$$

Before we describe the mechanism used to update $\underline{W}_j^n$ to $\underline{W}_j^{n+1}$ we look at the approximation $\tilde{\underline{g}}(\underline{w}^n)$ used for $\underline{g}(\underline{w})$.

Now, $\underline{g}(\underline{w}) = \begin{pmatrix} 0 \\ \frac{S'(r)}{S(r)} P \\ 0 \end{pmatrix}$ and we only need to approximate the second component. For this middle component $g_2(\underline{w})$ we notice first that, since the sound speed a is given by $a^2 = \frac{\gamma p}{\rho} = \frac{\gamma P}{R}$, we may therefore write

$$g_2(\underline{w}) = \frac{S'(r)}{S(r)} P = \frac{S'(r)}{S(r)} \frac{R a^2}{\gamma} = S'(r) \frac{\rho a^2}{\gamma} \quad .$$

The reason for doing this is that $g_2(\underline{w})$ now has a more "natural" approximation in the framework we have set up in the sense that $\hat{S}$ is averaged in the same way as R , i.e.

(†) By construction $\underline{F}_R - \underline{F}_L = \tilde{A}(\underline{W}_R - \underline{W}_L)$.

$$\tilde{g}_2(\underline{w}^n) = \frac{(\hat{S}_j - \hat{S}_{j-1})}{\Delta r} \quad \frac{\tilde{\rho}\tilde{a}^2}{\gamma} \qquad (3.$$

where $\tilde{a}^2$ is as before, and

$$\tilde{\rho} = \sqrt{\rho_L \rho_R} = \frac{\sqrt{R_L R_R}}{\sqrt{\hat{S}_L \hat{S}_R}} = \frac{\tilde{R}}{\tilde{S}} \quad .$$

We now project $\Delta_r \underline{F} = \underline{F}_j - \underline{F}_{j-1}$ and $\tilde{\underline{g}}(\underline{w}^n)$ from equations (3.12) onto the local eigenvectors given by equations (3.10) and update $\underline{w}_j^n$ to $\underline{w}_j^{n+1}$ as follows. Suppose

$$\Delta_r \underline{W} = \underline{W}_j - \underline{W}_{j-1} = \sum_{i=1}^{3} \alpha_i \underline{e}_i \qquad (3.$$

so that

$$\Delta_r \underline{F} = \sum_{i=1}^{3} \alpha_i \lambda_i \underline{e}_i \quad . \qquad (3.$$

Since $\tilde{A}$ has eigenvalues λ_i with corresponding eigenvectors $\underline{e}_i$, and

$$\tilde{\underline{g}}(\underline{w}^n) = -\frac{1}{\Delta r} \sum_{i=1}^{3} \beta_i \underline{e}_i \qquad (3.$$

we may write equations (3.12) as

$$\underline{w}_p^{n+1} = \underline{w}_p^n + \frac{\Delta t}{\Delta r} \sum_{i=1}^{3} \lambda_i \gamma_i \underline{e}_i \qquad (3.$$

where

$$\gamma_i = \alpha_i + \beta_i/\lambda_i \qquad (3.$$

and P may be L or R. To update $\underline{w}^n$ to $\underline{w}^{n+1}$ we use the method of upwind differencing, i.e. for each cell $[r_{j-1}, r_j]$ we add $\frac{\Delta t}{\Delta r} \lambda_i \gamma_i \underline{e}_i$ to $\underline{w}_j^n$ when $\lambda_i > 0$ and add $\frac{\Delta t}{\Delta r} \lambda_i \gamma_i \underline{e}_i$ to $\underline{w}_{j-1}^n$ when $\lambda_i < 0$, see Fig. 1.

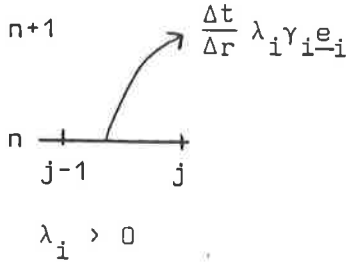

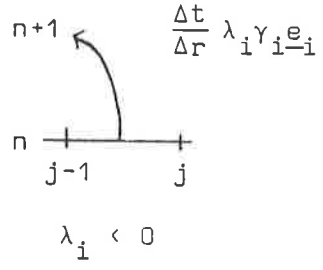

FIG. 1

This gives exact shock recognition for the Riemann problem given by equations (3.4) within the resolution of the grid provided that we use the previously defined local averages given by equations (3.7)-(3.8).

If we follow the algebra through, we obtain

$$\alpha_1 = \frac{1}{2\tilde{a}^2}\,(\Delta_r P + \tilde{R}\tilde{a}\Delta_r U) \qquad (3.2$$

$$\alpha_2 = \frac{1}{2\tilde{a}^2}\,(\Delta_r P - \tilde{R}\tilde{a}\Delta_r U) \qquad (3.2$$

$$\alpha_3 = \Delta_r R - \Delta_r P/\tilde{a}^2 \qquad (3.2$$

$$\beta_1 = \frac{\tilde{R}\Delta_r \hat{S}}{2\gamma\tilde{S}}\,((\gamma-1)u - \tilde{a}) \qquad (3.2$$

$$\beta_2 = \frac{\tilde{R}\Delta_r \hat{S}}{2\gamma\tilde{S}}\,((\gamma-1)u + \tilde{a}) \qquad (3.2$$

$$\beta_3 = -\frac{(\gamma-1)\tilde{R}\tilde{u}\Delta_r \hat{S}}{\gamma\tilde{S}} \qquad (3.2$$

(Note that the quantity $\Delta_r \hat{S}/\tilde{S}$ is independent of time, and therefore has to be worked out only once).

The expressions in equations (3.20) (a-f) have been written in terms of 'primitive' variables for simplicity and in doing so we have made use of the following identities

$$\Delta_r(RU) = \tilde{R}\Delta_r U + \tilde{U}\Delta_r R$$

$$\Delta_r(RU^2) = \tilde{U}^2\Delta_r R + 2\tilde{R}\tilde{U}\Delta_r U$$

We also note another identity, namely,

$$\tilde{a}^2 = \gamma\left(\frac{\tilde{P}}{\tilde{R}}\right) + \frac{(\gamma-1)\tilde{R}(\Delta-u)^2}{2(\sqrt{R_L} + \sqrt{R_R})^2} \qquad (3.$$

which ensures that $\tilde{a}^2$ is non-negative for real data. Moreover it gives conditions for the local sound speed to vanish, namely $\left(\frac{\tilde{P}}{\tilde{R}}\right) = 0$, $\Delta_r u = 0$, i.e. $p_L = p_R = 0$, $u_L = u_R$. This corresponds to special data for which we obtain equal wavespeeds, $\tilde{U}$ and equal eigenvectors $(1,\tilde{U},\frac{1}{2}\tilde{U}^2)^T$, so that in this case our scheme reduces to

$$\underline{W}_p^{n+1} - \underline{W}_p^n + \frac{\Delta t}{\Delta r}\,\tilde{U}\Delta_r R \begin{pmatrix} 1 \\ \tilde{U} \\ \frac{1}{2}\tilde{U}^2 \end{pmatrix} = \underline{0} \qquad (3.$$

representing an advancement of $\underline{W}_p^n$ entirely due to changes in the density profile. Although computationally this case would appear to be difficult to handle we notice that, when $\tilde{a} = 0$, by changing $\tilde{a}^2$ to a non-zero value the scheme reproduces equations (3.22). (The non-cartesian geometry is still present since $\underline{W} = S(r)\underline{w}$).

3.3 If we consider the special case of constant data $\rho_j^n = \rho^n$, $u_j^n = u^n$, $p_j^n = p^n$ for all j at time $t = n\Delta t$, equations (3.18)-(3.19) reduce to

$$\frac{\underline{W}_j^{n+1} - \underline{W}_j^n}{\Delta t} + \frac{\Delta_r \hat{S}}{\Delta r} \begin{pmatrix} \rho^n u^n \\ \rho^n (u^n)^2 \\ u^n (e^n + p^n) \end{pmatrix} = 0 \qquad (3.2$$

giving a direct finite difference analogue of equations (2.31)-(2.32) with $\underline{u}_r = \underline{0}$ (corresponding to $\Delta_r \underline{u} = 0$). Equations (3.23) have the solution

$$\rho_j^{n+k} = \rho^n \left(1 - \frac{\Delta t u^n \Delta_r \hat{S}}{\Delta r \tilde{S}}\right)^k \qquad (3.24a$$

$$u_j^{n+k} = u^n \qquad (3.24b$$

$$p_j^{n+k} = p^n \left(1 - \frac{\Delta t \gamma u^n \Delta_r \hat{S}}{\Delta r \tilde{S}}\right)^k \qquad (3.24c$$

for $k \geq 0$, which are approximate solutions to the exact solutions of equations (2.31)-(2.32) with this given data, namely

$$\rho(j\Delta r, (n+k)\Delta t) = \rho^n e^{-k\Delta t u^n \frac{S'(r)}{S(r)}} \qquad (3.2$$

$$u(j\Delta r, (n+k)\Delta t) = u^n \qquad (3.$$

$$p(j\Delta r, (n+k)\Delta t) = p^n e^{-k\Delta t \gamma u^n \frac{S'(r)}{S(r)}} \qquad (3.2$$

In particular, with $u^n = 0$, no flow and constant density and pressure, ρ^n, p^n, respectively, equations (3.24)(a-c) yield the correct physical solution namely $u^{n+k} = 0$, $\rho^{n+k} = \rho^n$, $p^{n+k} = p^n$.

To solve equations (2.27)-(2.30) using the finite difference approximation given by equations (3.18)-(3.19) we use the method of upwind differencing on the three waves with wavespeeds $\lambda_1, \lambda_2, \lambda_3$ and wavestrengths $\gamma_1, \gamma_2, \gamma_3$ (which will differ from the usual wavestrengths in slab symmetry due to the variation of $S(r)$). This gives the first order approximation mentioned earlier. We can then calculate second order corrections by transferr fractions of the increments described in Fig. 1. If we limit these transfers using a suitable flux limiter or B-function, [2,3,4], our scheme will be second order almost everywhere, oscillation free, and will sharpen up certain features that will be smeared by using the first order method only.

In addition, we can easily incorporate into the scheme a device to disperse entropy-violating solutions and treat expansion fans correctly. This is done by considering the one-sided scheme described in Fig. 1 as a two-sided scheme, sending increments to both ends of a cell, (see [7]).

In the next section we note the properties of the scheme described in relation to the type of problem we wish to solve.

4. PROPERTIES OF THE SCHEME

In this section we briefly discuss two properties of the scheme proposed here for solving equations (2.27)-(2.30) in relation to the features that we expect to occur in this type of problem.

(i) The scheme is 'conservative' in the following sense. Equations (2.27) and (2.29) represent conservation of mass $\rho S(r)dr$ and energy $eS(r)dr$, but conservation of momentum $\rho u\, S(r)\, dr$ is not maintained in equation (2.28). This is because the pressure term arises as $S(r)p_r$ which is not derivable from a potential, however, $(S(r)p)_r$ is derivable from a potential, but leads to a non-zero right-hand side term $S'(r)p$ (since in the non-Cartesian case $S \not\equiv 1$). Thus, integrating equations (2.33) gives

$$\frac{\partial}{\partial t}\left(\int_{r_{j-1}}^{r_j} \underline{W} dr\right) = -\underline{F}(\underline{w})\Big|_{r_{j-1}}^{r_j} + \begin{pmatrix} 0 \\ \int_{r_{j-1}}^{r_j} S'(r)p\,dr \\ 0 \end{pmatrix} \qquad (4.$$

Therefore, in the region $0 \leq r \leq 1$

$$\frac{\partial}{\partial t}\left(\int_0^1 \underline{W}\, dr\right) = -(\underline{F}_1 - \underline{F}_0) + \begin{pmatrix} 0 \\ \int_0^1 S'(r)p\,dr \\ 0 \end{pmatrix} \qquad (4.2$$

Thus, the first and last components of $\underline{W}$ are conserved, and if $S'(r) \equiv 0$, so is the middle component.

We now show that the scheme given by equations (3.18)-(3.19) is 'conservative' in a finite difference sense. Since, by construction $\tilde{A}\, \Delta_r \underline{W} = \Delta_r \underline{F}$ we have

$$\underline{W}_j^{n+1} = \underline{W}_j^n - \frac{\Delta t}{\Delta r} \Delta_r \underline{F} + \Delta t \begin{pmatrix} 0 \\ \tilde{g}_2(\underline{w}^n) \\ 0 \end{pmatrix} \qquad (4.3)$$

Thus

$$\sum_j \underline{W}_j^{n+1} = \sum_j \underline{W}_j^n - \frac{\Delta t}{\Delta r}(\underline{F}_N - \underline{F}_0) + \begin{pmatrix} 0 \\ \Delta t \sum_j g_2(\underline{w}^n) \\ 0 \end{pmatrix} \qquad (4.4)$$

where $N\Delta r = 1$. Thus, our finite difference scheme is 'conservative' in the sense that the first and last components of $\underline{W}^n$ are conserved, and the second component will be conserved if $S'(r) \equiv 0$, i.e. $\Delta_r \hat{S} = 0$, i.e. $\hat{g}_2(\underline{W}^n) = 0$.

(ii) The scheme also 'recognises' shock-waves. By this we mean $\Delta_r \underline{F} = s\Delta_r \underline{W}$ for some scalar shock speed s. By equations (3.15)-(3.16) s is an eigenvalu of $\tilde{A}$. A projection of $\Delta_r \underline{W}$ onto the local eigenvectors of $\tilde{A}$ will be solely onto the eigenvector which corresponds to s. In this special case, the solution of the linearised Riemann problem given by equations (3.5), is exact.

The reason that this formulation alone recognises shocks is that the right hand side term $\underline{g}(\underline{w})$ does not contribute to the shock wave, essentia because it does not contain any derivatives in $\underline{w}$, and therefore no jumps. In particular, suppose that the pressure p jumps from p_L to p_R at $r = r_0$, then

$$\lim_{\varepsilon\to 0} \int_{r_0-\varepsilon}^{r_0+\varepsilon} S'(r)p\,dr = \lim_{\varepsilon\to 0} (p_L(S(r_0)-S(r_0-\varepsilon)) + p_R(S(r_0+\varepsilon)-S(r_0))) = 0$$

since $S(r)$ is continuous, Thus,

$$\lim_{\varepsilon\to 0} \int_{r_0-\varepsilon}^{r_0+\varepsilon} \underline{g}(\underline{w})\,dr = \underline{0} \quad , \tag{4.}$$

i.e. the shock speed is given by $\dfrac{[\underline{F}(\underline{W})]}{[\underline{W}]}$, with the right hand side making no contribution. Moreover, in terms of the three scalar problems obtained by diagonalising the system given by equations (3.5) with A a constant matrix, we have

$$\frac{\partial V_i}{\partial t} + \lambda_i \frac{\partial V_i}{\partial r} = h_i(\underline{w}) \qquad i = 1,2,3 \tag{4.6}$$

where

$$\underline{V} = X^{-1}\underline{W} \ , \quad \underline{h} = X^{-1}\underline{g} \ ,$$

and X is the modal matrix consisting of the eigenvectors of A with eigenvalues λ_i. Solutions to equations (4.6) can be represented in terms of a

'shock solution', this being a solution of the homogeneous equation, i.e. equations (4.6) with $\underline{h}(\underline{w}) = \underline{0}$, and a 'source solution', being the particular solution of the inhomogeneous equations (4.6). In terms of our scheme, we effectively solve equations (4.6) approximately, and thus the important 'shock solution' is modelled as a consequence of the construction of $\tilde{A}$.

In the next section we discuss two test problems that can be used to test algorithms for solving equations (2.27)-(2.30).

5. TEST PROBLEMS

In this section we look at two test problems used to test the previously described algorithm for solving equations (2.27)-(2.30).

Problem 1

The first problem is concerned with infinite shock reflection, and can be posed in slab, cylindrical or spherical symmetry, denoted by $d = 1$, 2 or 3, respectively.

We consider a region $0 \leq r \leq 1$ with initial conditions

$$\rho(r,0) = 1$$

$$u(r,0) = -1$$

$$p(r,0) = 0$$

i.e. low energy gas (zero temperature) moving towards $r = 0$. This represents shock reflection from a rigid wall ($d = 1$), an axis of symmetry ($d = 2$), or the centre of a sphere ($d = 3$), all at $r = 0$. The gas is brought to rest at $r = 0$, and denoting (0) initial values, $(-)$ pre-shocked values, and $(+)$ post-shocked values, we have

$$\rho^0 = 1, \quad \rho^- = \left(\frac{\gamma+1}{\gamma-1}\right)^{d-1} \rho^0, \quad \rho^+ = \left(\frac{\gamma+1}{\gamma-1}\right)\rho^- \tag{5.1a}$$

$$u^0 = -1, \quad u^- = -1, \quad u^+ = 0 \tag{5.1b}$$

$$p^0 = 0, \quad p^- = 0, \quad p^+ = \frac{(\gamma-1)}{2}\rho^+ \tag{5.1c}$$

and

$$\rho = (1 + t/r)^{d-1}, \quad u = -1, \quad p = 0 \quad \text{for} \quad r/t \geq \frac{(\gamma-1)}{2} \; . \tag{5.1d}$$

The shock moves out from the origin with speed $\frac{(\gamma-1)}{2}$. (N.B. $p^-/\rho^- = \infty$).

Taking the spherical case as example with $d = 3$ and $\gamma = 5/3$ (a monotonic gas), the solution at $t = 0.6$ is given in Fig. 2.

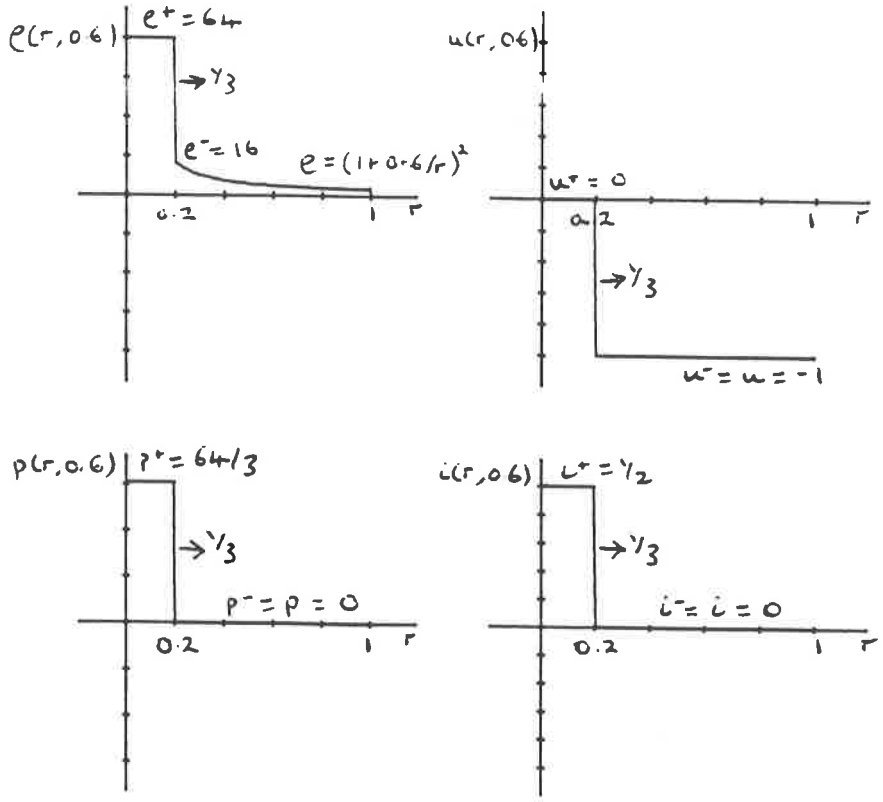

FIG. 2

The case $d = 1$ is a standard test problem in shock reflection, and the solution is not difficult to compute. However, the cases $d = 2$ and $d = 3$ are much more difficult to model (See Noh [5]).

It is the last case, $d = 3$, that we concentrate on here i.e. a spherically infinite diverging shock, for various γ's. (N.B. $S(r) = r^2$).

Problem 2

The second test problem is concerned with a converging cylindrical shock. Here, we consider a region $0 \leq r \leq 200$ for the cylindrically symmetric case given by equations (2.27)-(2.30) with $S(r) = r$.

Initially, a cylindrical diaphragm of radius $r = 100$ separates two uniform regions of an ideal gas at rest ($\gamma = 1.4$, i.e. a diatomic gas, e.g. air) The initial conditions are $p = \rho = 4$ in the outer region, and $p = \rho = 1$ in the inner region. When the diaphragm is removed at $t = 0$, a converging shock

wave followed by a converging contact discontinuity move towards the axis, $r = 0$, and a diverging rarefaction wave moves outwards.

The shock accelerates as it approaches the axis of symmetry, is reflected from the axis, interacts with the contact discontinuity (still converging), which results in a transmitted shock, a converging contact discontinuity, and a weak converging reflected shock. This problem has been treated by Ben-Artzi and Falcovitz [6] using a more complicated Riemann solver. In the next section we display the numerical results for the two problems described above.

6. NUMERICAL RESULTS

In this section we exhibit the numerical results obtained for the two test problems described in §5 using the scheme described in §3. In both cases we apply a reflection condition† at $r = 0$.

Problem 1

Figures 1-6 refer to Problem 1 using either first order, or second order with the 'Minmod' limiter or the 'Superbee' limiter (see Sweby [4]). We vary the ratio of specific heat capacities γ and the output times but the number of mesh points remains fixed at 100.

Figure 1	$\gamma = 5/3$	$t = 0.6$	First order
Figure 2	$\gamma = 5/3$	$t = 0.6$	Superbee limiter
Figure 3	$\gamma = 5/3$	evolution to $t = 0.6$	Superbee limiter
Figure 4	$\gamma = 1.4$	$t = 0.9$	First order
Figure 5	$\gamma = 1.4$	$t = 0.9$	Minmod limiter
Figure 6	$\gamma = 1.4$	evolution to $t = 0.9$	Minmod limiter

---

(†) A reflected boundary condition at the left hand end can be implemented by considering an 'image' cell at the boundary and imposing equal density and pressure, and equal and opposite velocity at either end of the cell. This results in no net movement in the cell. A similar argument applies for a rig hand reflected boundary condition.

We note that because the incoming flow at $r = 1$ is supersonic we have imposed the exact solution there: however, this condition can easily be replaced by introducing a low energy gas at the right hand end.

Problem 2

Figures 7-12 refer to Problem 2 using the second order scheme with the 'Superbee' limiter. We have used $\gamma = 1.4$ and 200 mesh points.

Figure 7	t = 54	the converging shock approaches r = 0
Figure 8	t = 56	the shock is about to hit the axis
Figure 9	t = 58	the shock has been reflected from the axis
Figure 10	t = 70	the diverging shock, (followed by a rarefaction wa is headed towards the converging contact discontin
Figure 11	t = 90	the interaction of the shock and contact discontin
Figure 12	t = 110	the interaction results in a diverging transmittec shock, a converging contact discontinuity and a we converging shock

For Problem 1 we note the extremely good representation of the solution, and propagation of the shock in time. Although it is a simple test problem, it has been found difficult to achieve good results (see Noh [5]). Since the only feature in the the solution is a shock discontinuity, the first order method works well, with a slight lack of resolution in the smooth part of the flow.

For Problem 2 we have found that the first order method is not as accurate since the solution has a number of features that require good resolutic However, the second order scheme applied with the Superbee limiter compares well with the solutions computed by Ben-Artzi and Falcovitz [6], especially the weak converging shock present at $t = 110$.

The c.p.u. time required to compute the results on an Amdahl V/7A was found to be as follows:-

(i) Problem 1, with 'Superbee' and 100 mesh points takes 0.0157 c.p.u. seconds to compute one time step, and a total of 1.256 c.p.u. seconds to reach a real time of 0.6 s using 80 time steps.

(ii) Problem 2, with 'Superbee' and 200 mesh points takes 0.04 c.p.u. seconds to compute one time step and a total of 8.64 c.p.u. seconds to reach a real time of 54 s using 216 time steps. The reason for the amount of c.p.u. time used per time step per mesh point being higher in Problem 2 is that we needed to include the entropy modification mentioned in §3.

A minor modification to our algorithm allows for a variable (adaptive) time step and gives the ability to decrease the total amount of computing time used.

SOLUTION OF THE EULER EQUATIONS WITH SPHERICAL SYMMETRY - A Spherically Infinite Diverging Shock

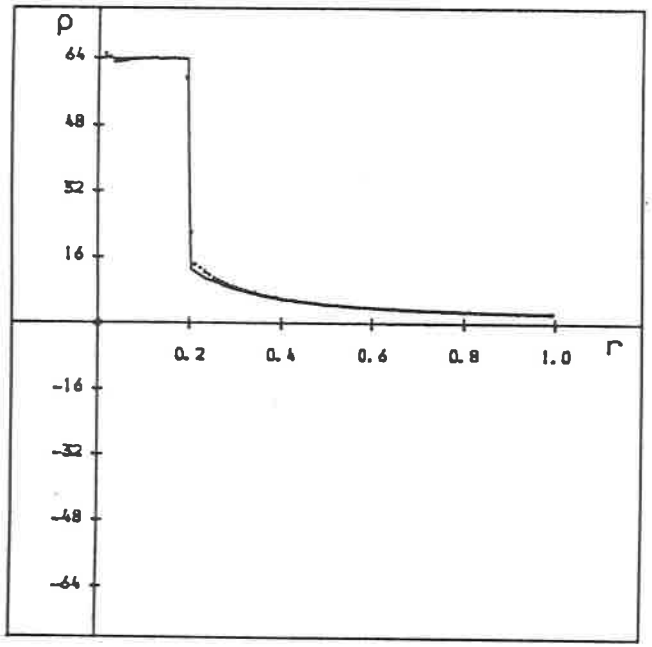

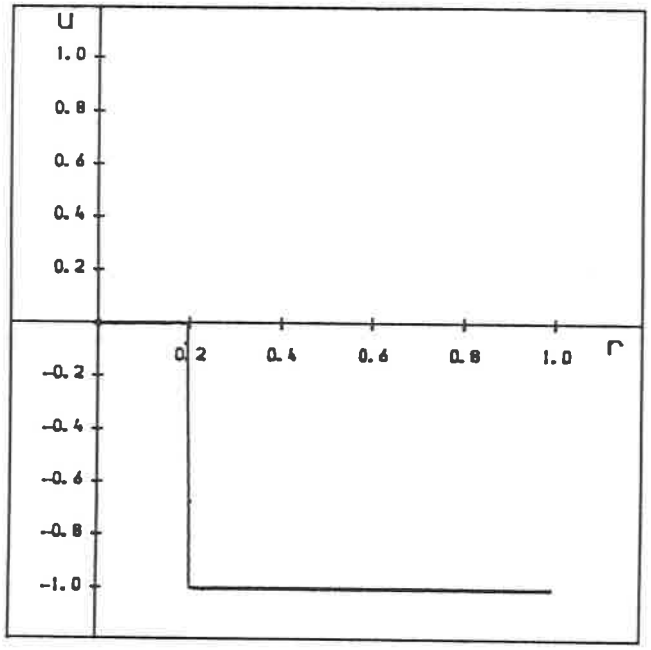

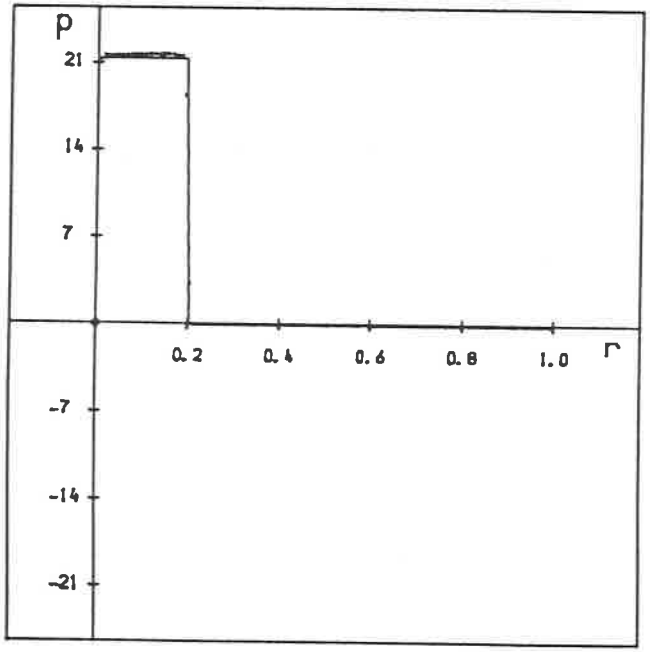

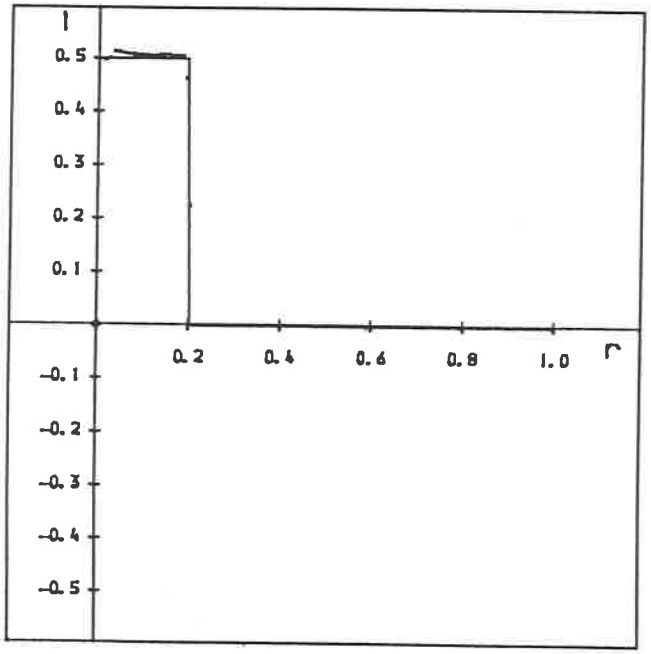

At time t = 0.6 s

FIG. 1

KEY

ρ - Density
u - Velocity
p - Pressure
I - Internal energy

—— Exact solution
..... Approximate solution

PARAMETERS

$\gamma = 5/3$
100 Mesh points
80 Time steps
$\Delta r = 0.01$
$\Delta t = 0.0075$
No limiter used

INITIAL CONDITIONS

$\rho = 1$
$u = -1$
$p = 0$
$\}$ $0 < r < 1$

Reflected Boundary Conditions at r=0

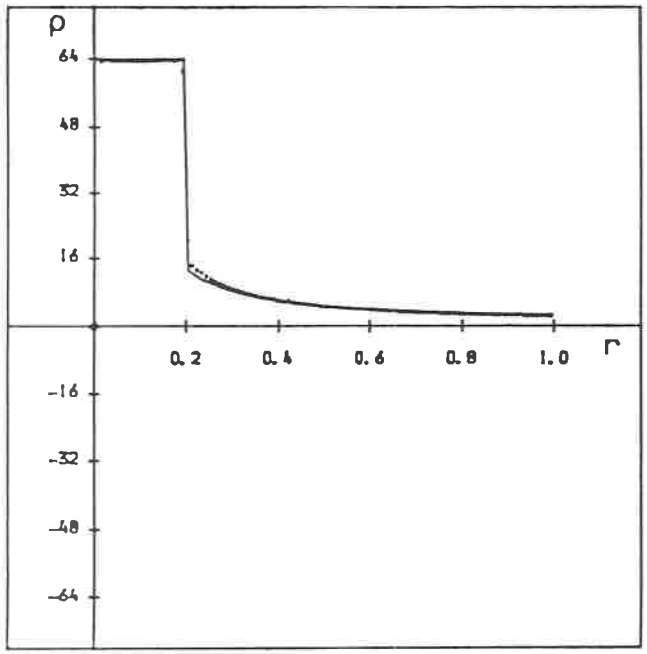

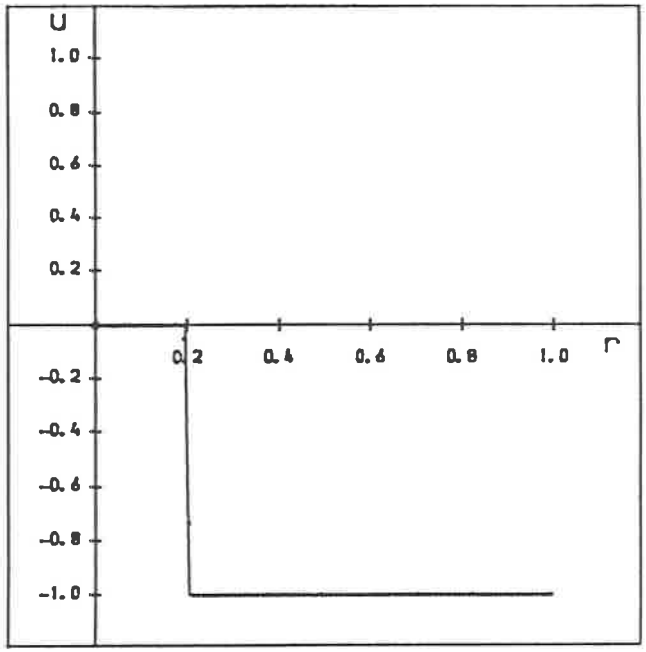

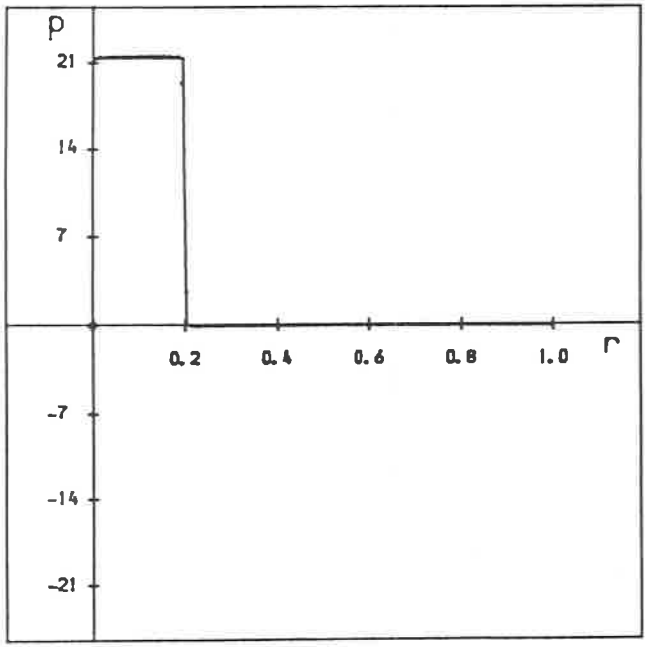

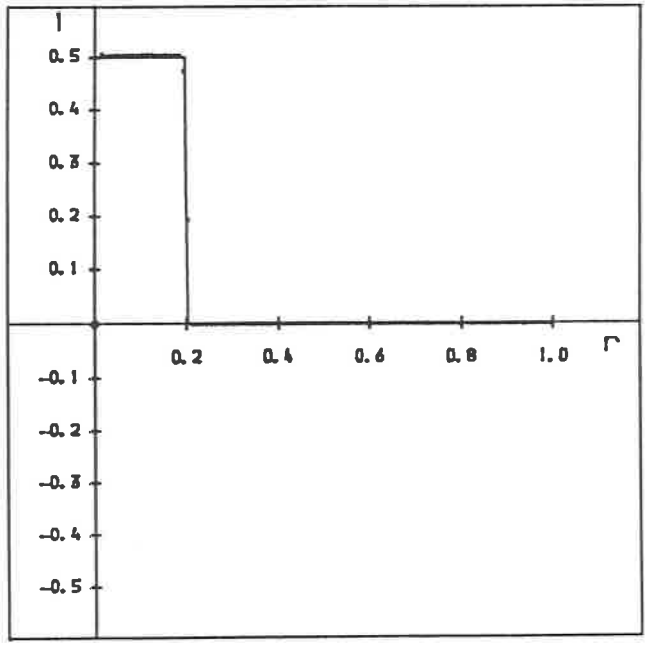

KEY

ρ – Density
u – Velocity
p – Pressure
I – Internal energy

—— Exact solution
..... Approximate solution

PARAMETERS

$\gamma = 5/3$
100 Mesh points
100 Time steps
$\Delta r = 0.01$
$\Delta t = 0.006$
'Superbee' limiter used

INITIAL CONDITIONS

$\left.\begin{array}{l} \rho = 1 \\ u = -1 \\ p = 0 \end{array}\right\}$ $0 < r < 1$

Reflected Boundary Conditions at r=0

At time t = 0.6 s

FIG. 2

SOLUTION OF THE EULER EQUATIONS WITH SPHERICAL SYMMETRY - A Spherically Infinite Diverging Shock

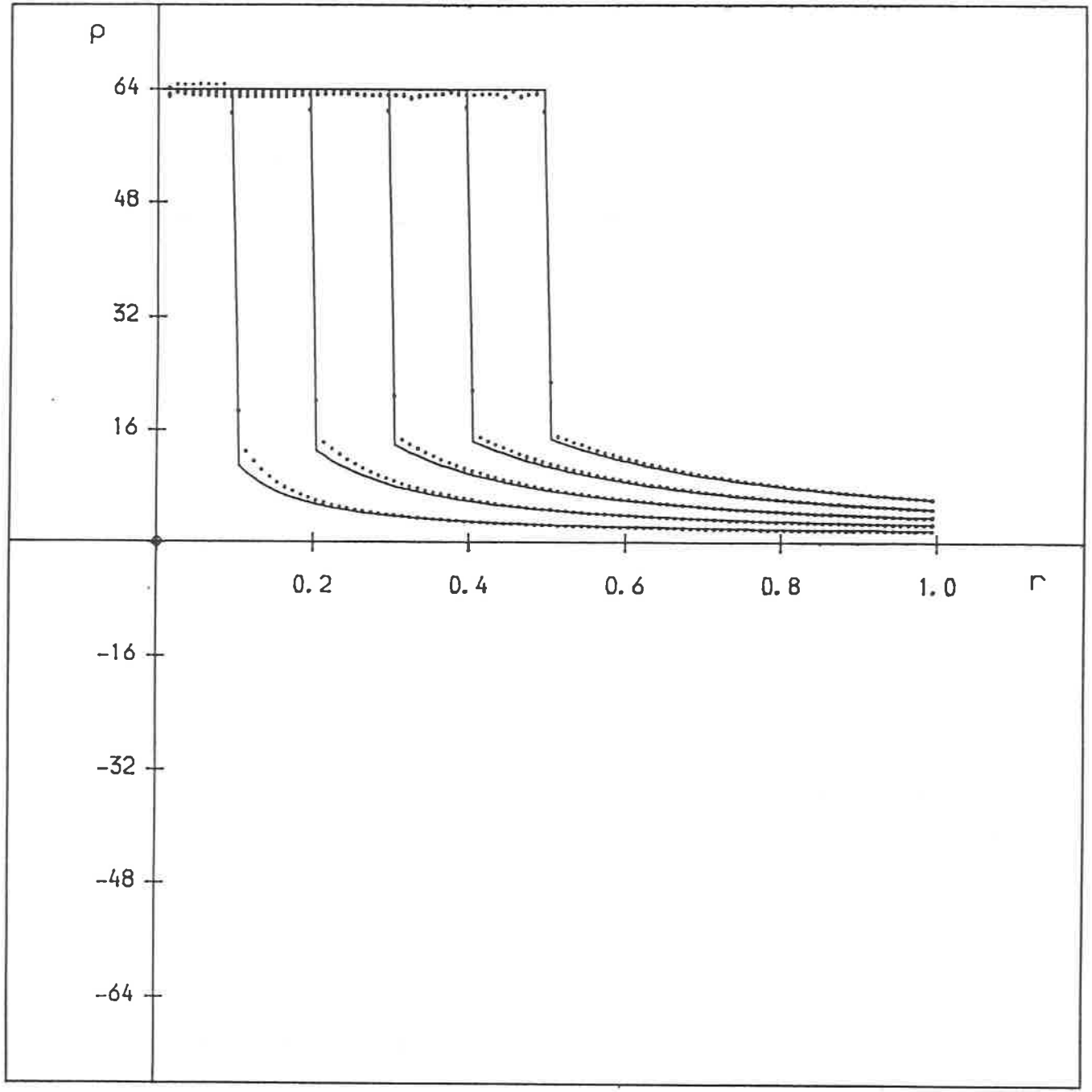

The solution at times t = 0.3, 0.6, 0.9, 1.2, 1.5 s FIG. 3

KEY

ρ - Density

—— Exact solution at intervals of 0.3 s

..... Approximate solution at intervals of 0.3 s

PARAMETERS

$\gamma = 5/3$

100 Mesh points

50-250 Time steps

$\Delta r = 0.01$

$\Delta t = 0.006$

'Superbee' limiter used

INITIAL CONDITIONS

$\rho = 1$
$u = -1$ } $0 < r < 1$
$p = 0$

Reflected Boundary Conditions at r=0

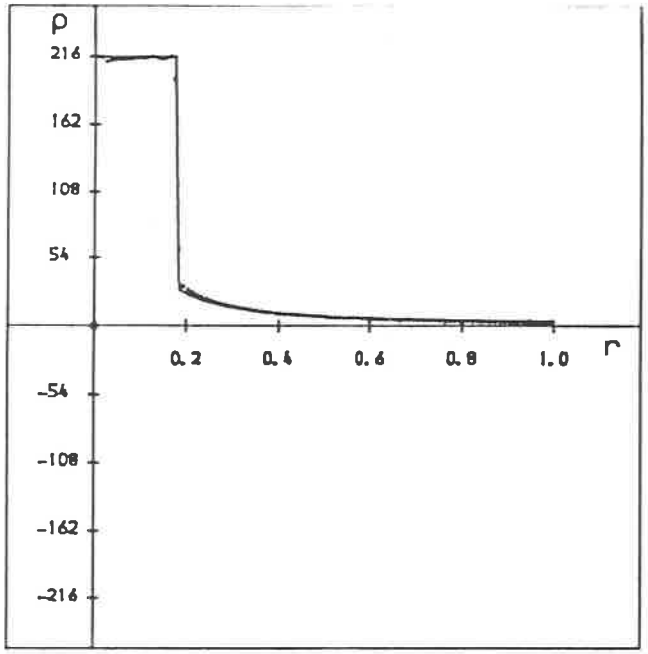

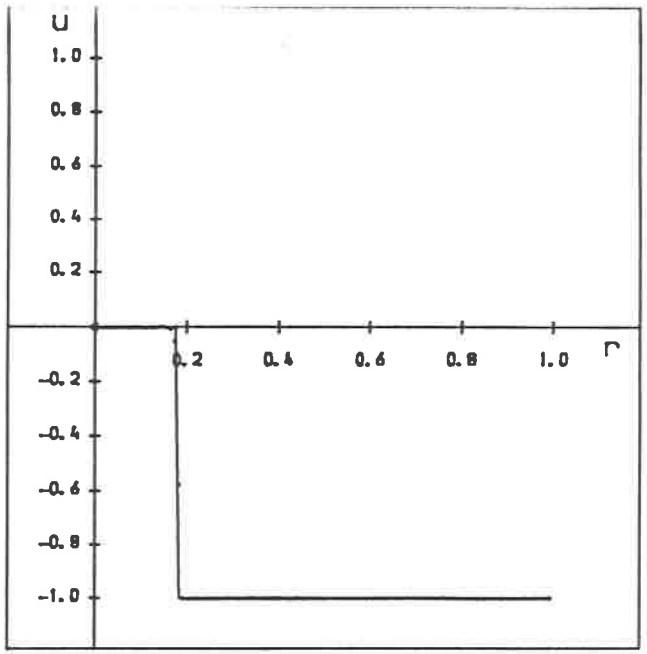

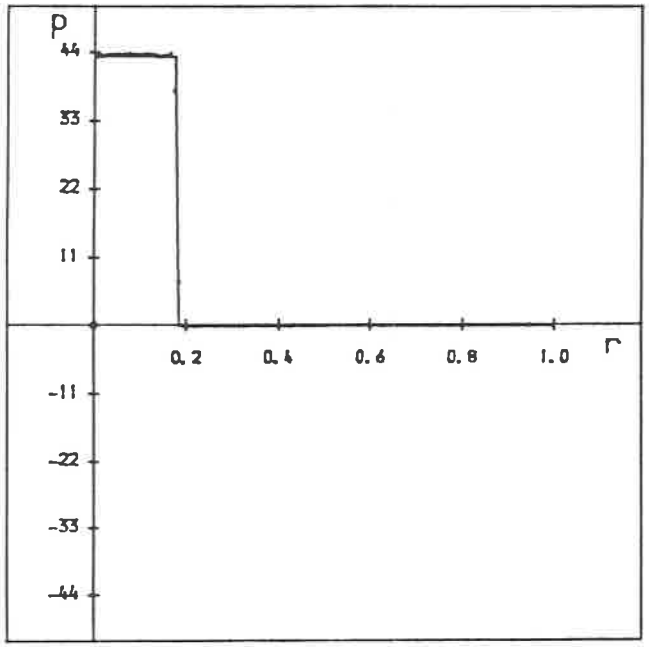

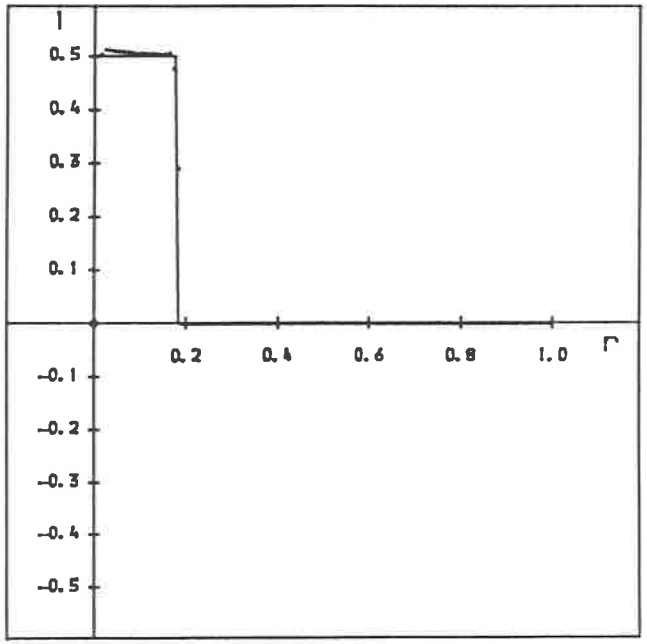

KEY

p – Density
u – Velocity
p – Pressure
I – Internal energy

—— Exact solution
..... Approximate solution

PARAMETERS

$\gamma = 1.4$
100 Mesh points
150 Time steps
$\Delta r = 0.01$
$\Delta t = 0.006$
No limiter used

INITIAL CONDITIONS

$\left.\begin{array}{l} \rho = 1 \\ u = -1 \\ p = 0 \end{array}\right\}$ $0 < r < 1$

Reflected Boundary Conditions at r=0

At time t = 0.9 s

FIG. 4

SOLUTION OF THE EULER EQUATIONS WITH SPHERICAL SYMMETRY - A Spherically Infinite Diverging Shock

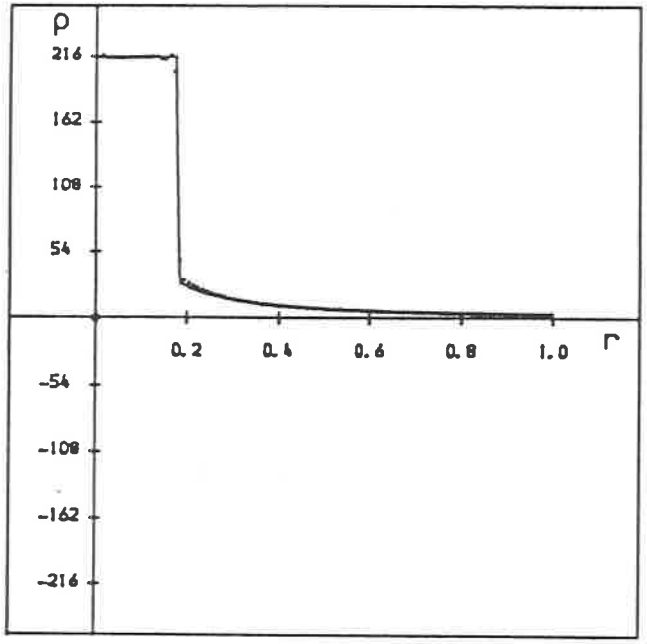

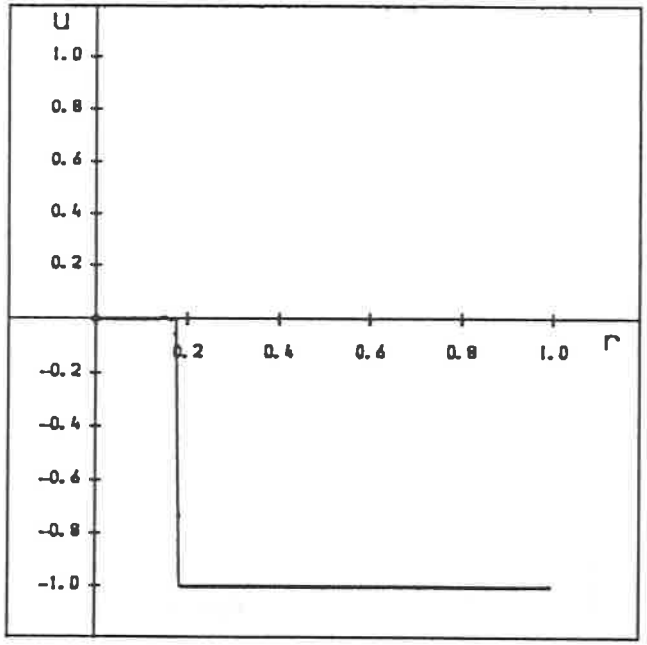

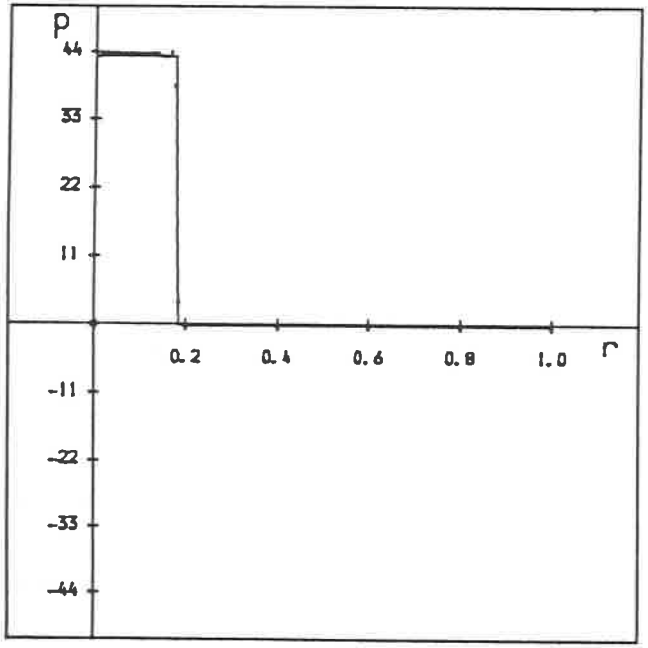

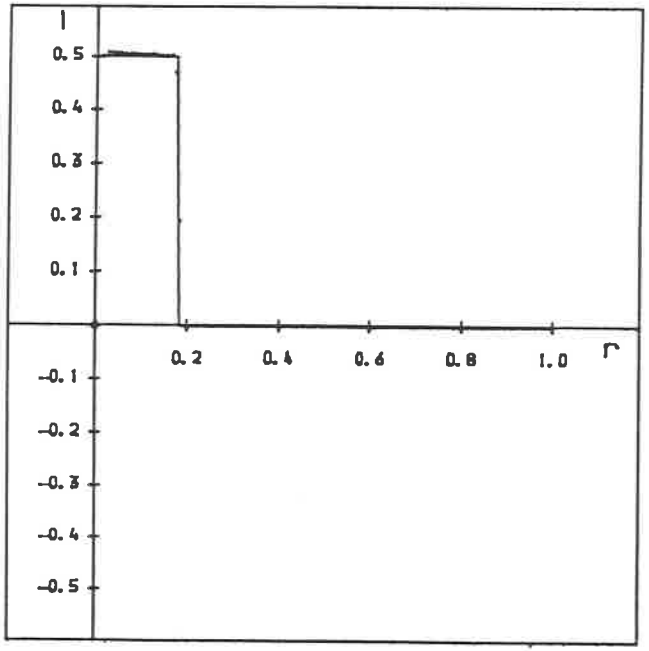

At time t = 0.9 s

FIG. 5

KEY

ρ - Density
u - Velocity
p - Pressure
I - Internal energy

—— Exact solution
..... Approximate solution

PARAMETERS

$\gamma = 1.4$
100 Mesh points
150 Time steps
$\Delta r = 0.01$
$\Delta t = 0.006$
'Minmod' limiter used

INITIAL CONDITIONS

$\rho = 1$
$u = -1$
$p = 0$
$0 < r < 1$

Reflected Boundary Conditions at r=0

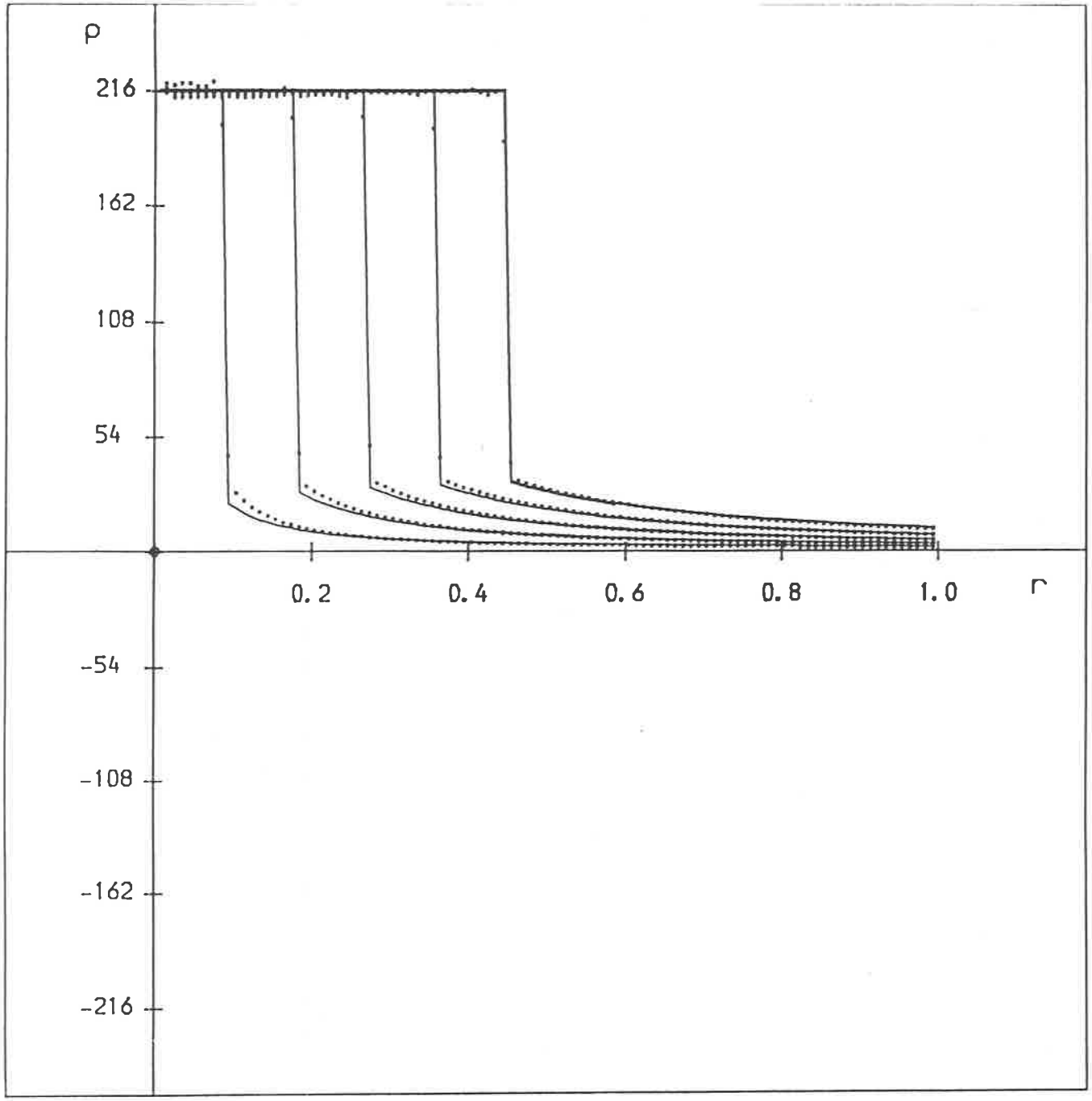

The solution at times t = 0.45, 0.9, 1.35, 1.8, 2.25 s

FIG. 6

KEY

ρ - Density

—— Exact solution at intervals of 0.45 s

..... Approximate solution at intervals of 0.45 s

PARAMETERS

$\gamma = 1.4$

100 Mesh points

75-375 Time steps

$\Delta r = 0.01$

$\Delta t = 0.006$

'Minmod' limiter used

INITIAL CONDITIONS

$\left.\begin{array}{l} \rho = 1 \\ u = -1 \\ p = 0 \end{array}\right\}$ $0 < r < 1$

Reflected Boundary Conditions at r=0

SOLUTION OF THE EULER EQUATIONS WITH CYLINDRICAL SYMMETRY - A Converging Cylindrical Shock

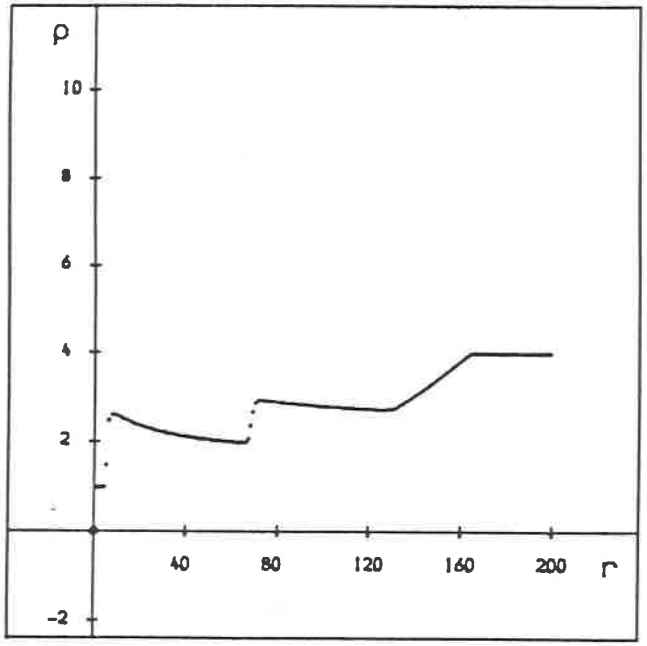

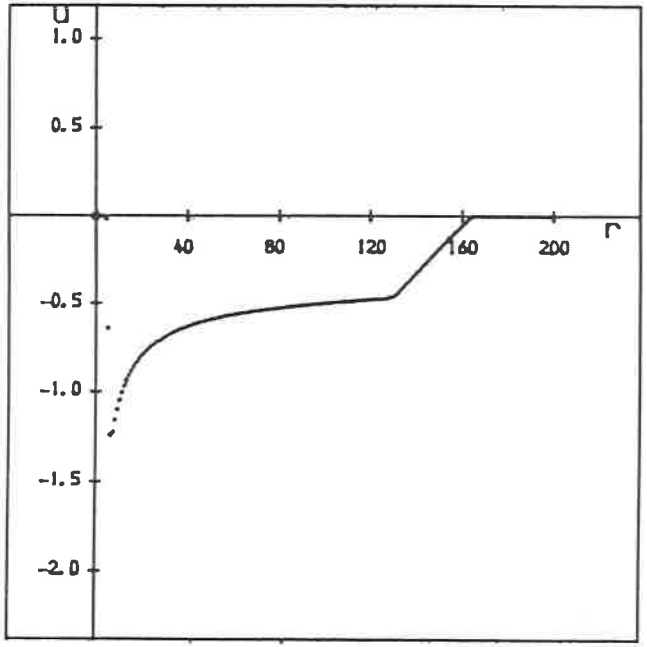

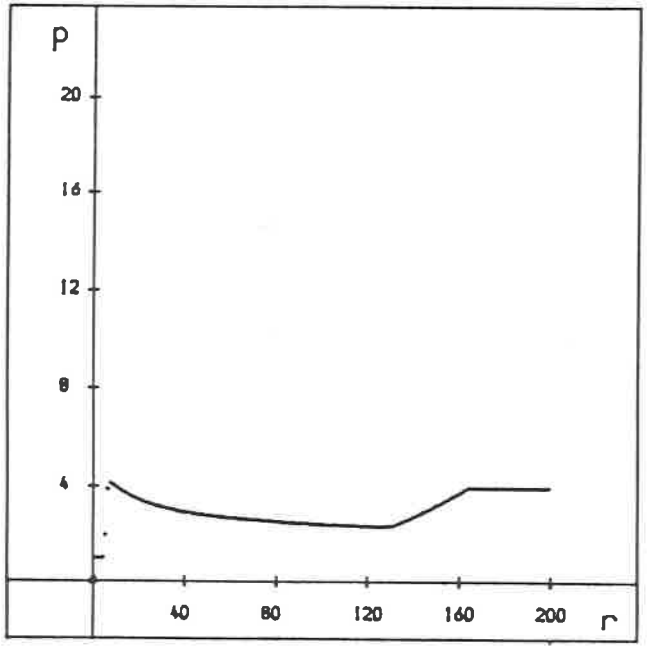

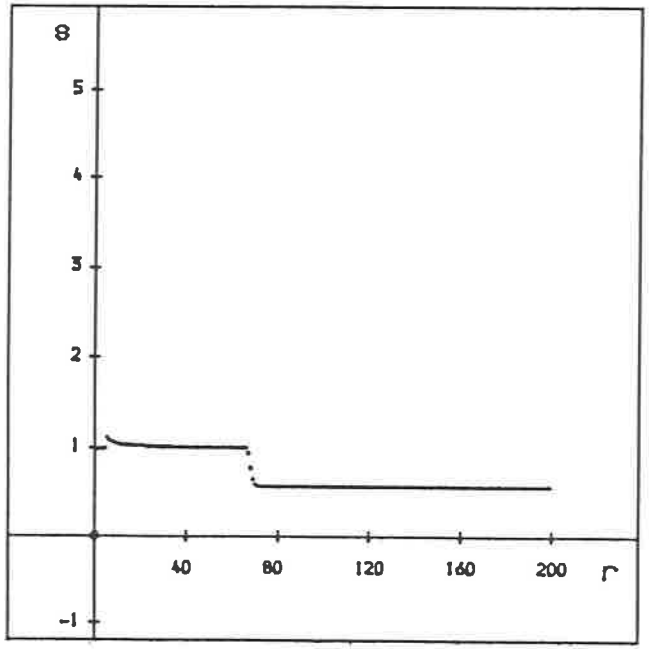

KEY

ρ - Density
u - Velocity
p - Pressure
s - Entropy

..... Approximate solution

PARAMETERS

$\gamma = 1.4$
200 Mesh points
216 Time steps
$\Delta r = 1$
$\Delta t = 0.25$
'Superbee' limiter used

INITIAL CONDITIONS

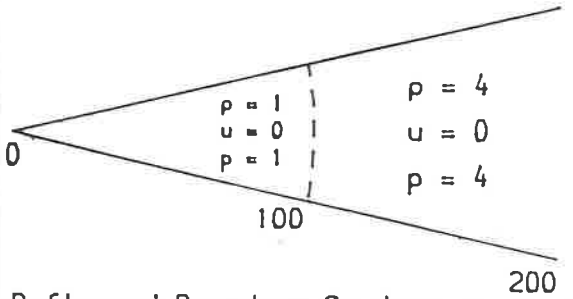

Reflected Boundary Conditions at r=0

At time t = 54 s

FIG. 7

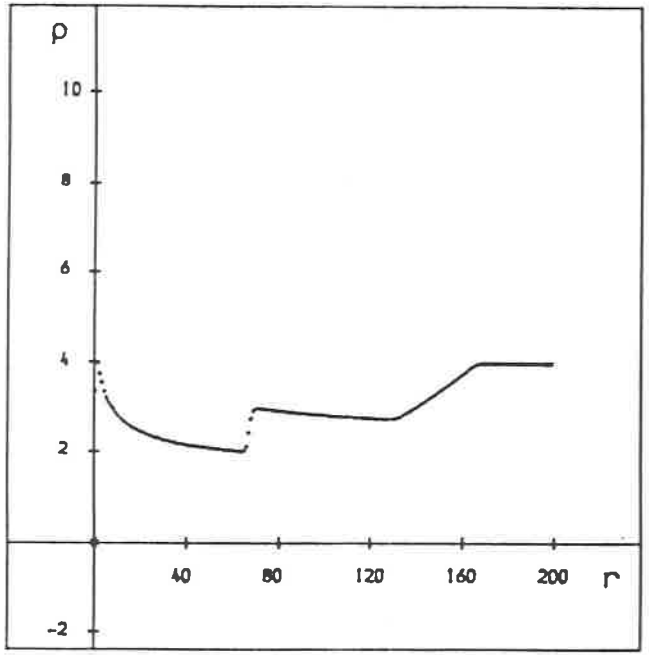

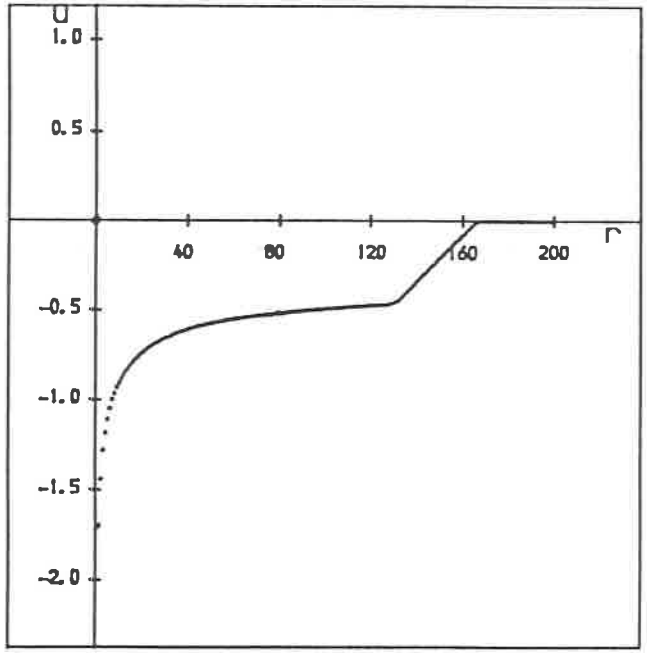

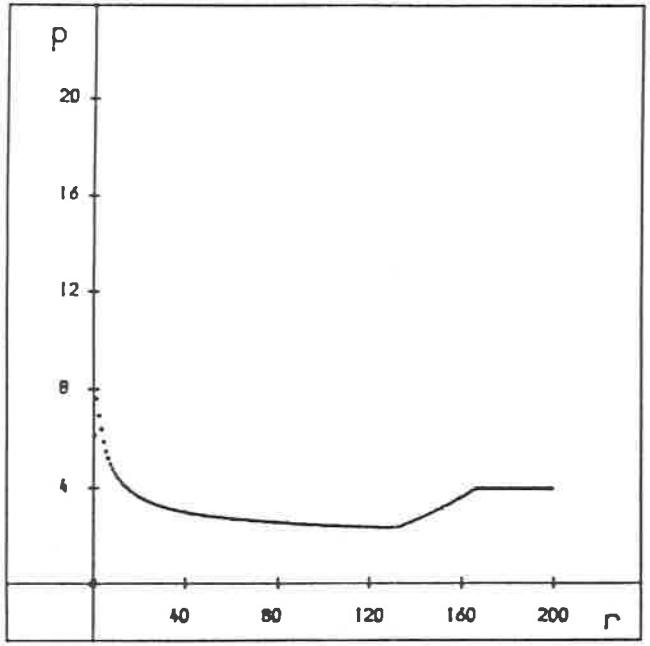

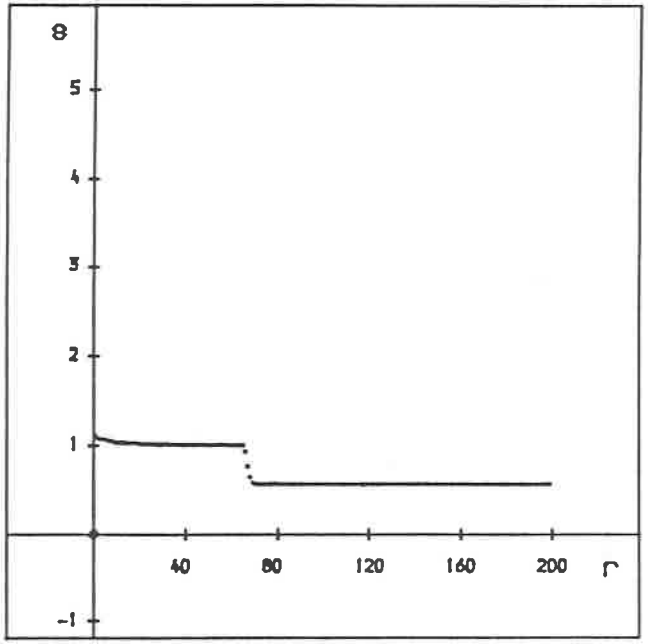

KEY

p - Density
u - Velocity
p - Pressure
s - Entropy

..... Approximate solution

PARAMETERS

$\gamma = 1.4$
200 Mesh points
224 Time steps
$\Delta r = 1$
$\Delta t = 0.25$
'Superbee' limiter used

INITIAL CONDITIONS

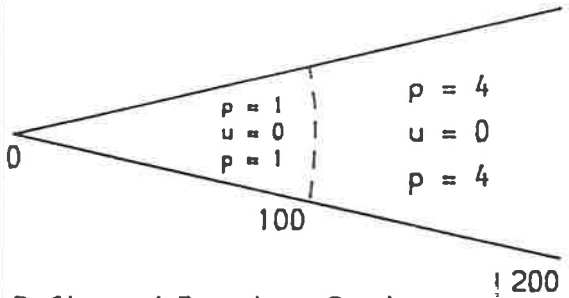

Reflected Boundary Conditions at r=0

At time t = 56 s

FIG. 8

SOLUTION OF THE EULER EQUATIONS WITH CYLINDRICAL SYMMETRY - A Converging Cylindrical Shock

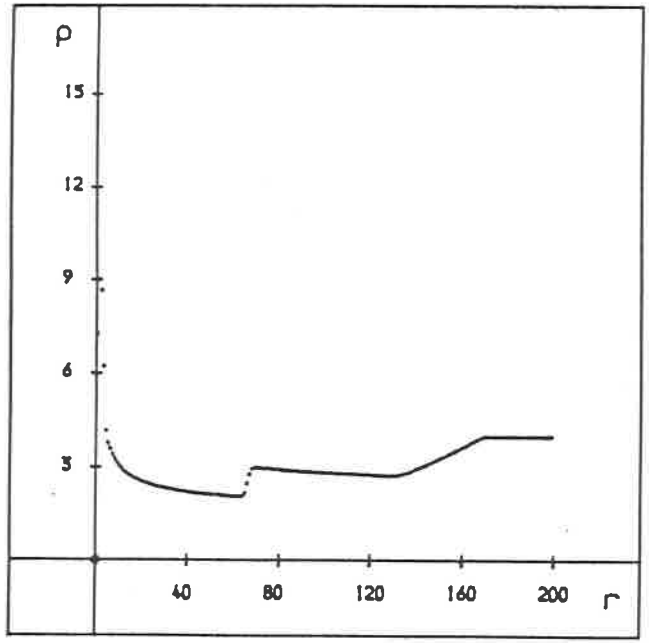

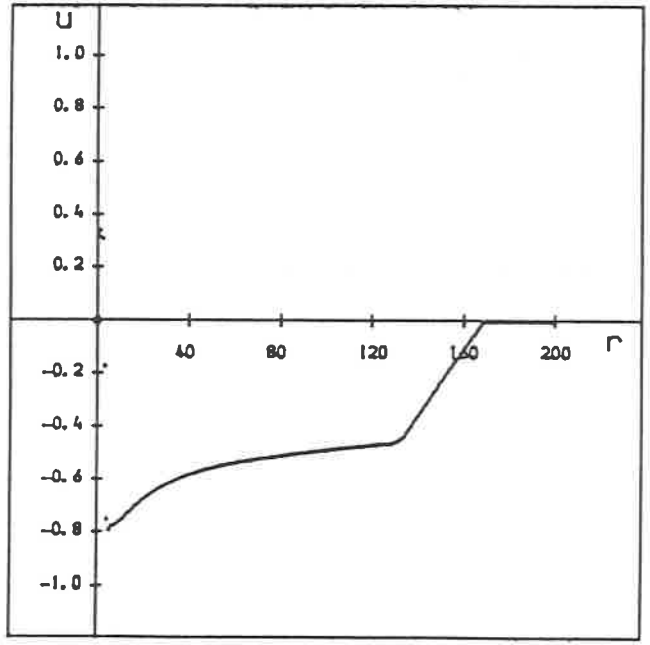

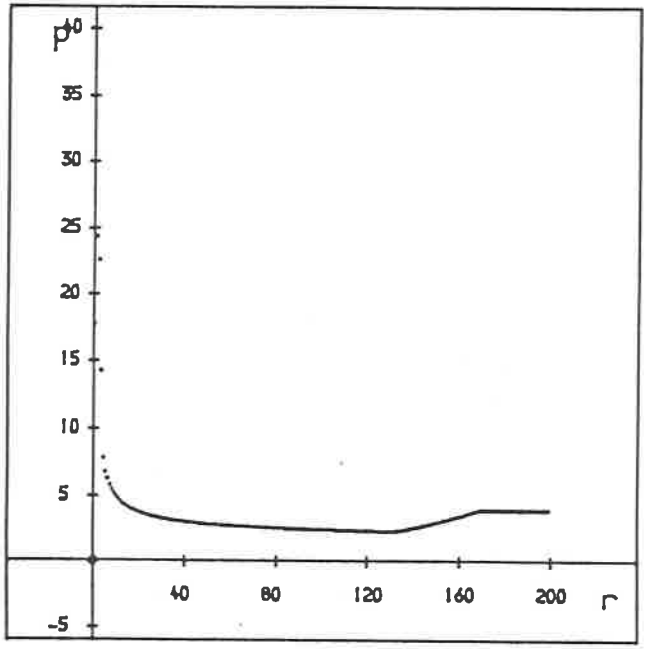

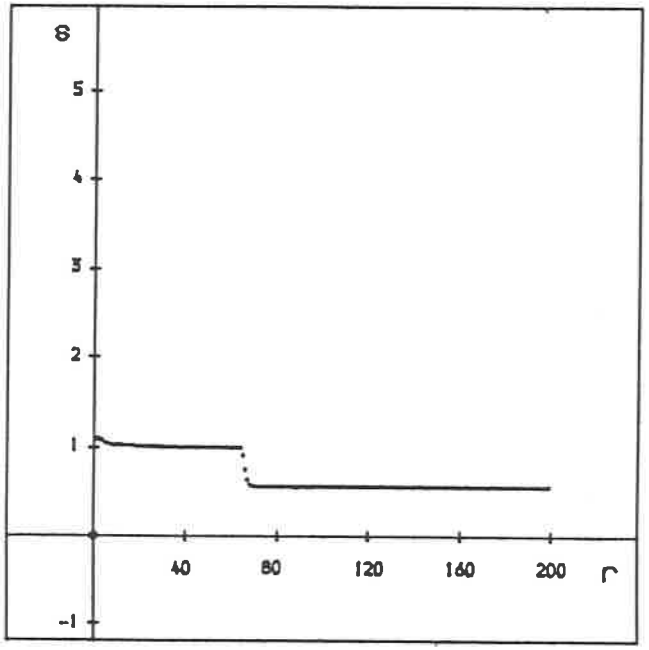

KEY

ρ - Density
u - Velocity
p - Pressure
s - Entropy

..... Approximate solution

PARAMETERS

γ = 1.4
200 Mesh points
232 Time steps
Δr = 1
Δt = 0.25
'Superbee' limiter used

INITIAL CONDITIONS

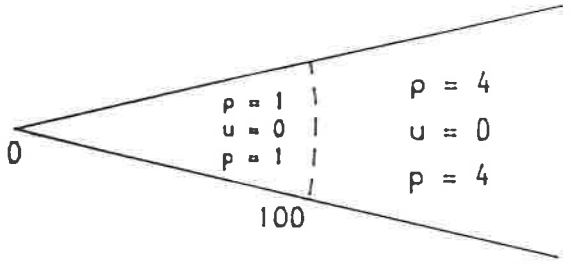

Reflected Boundary Conditions at r=0

At time t = 58 s

FIG. 9

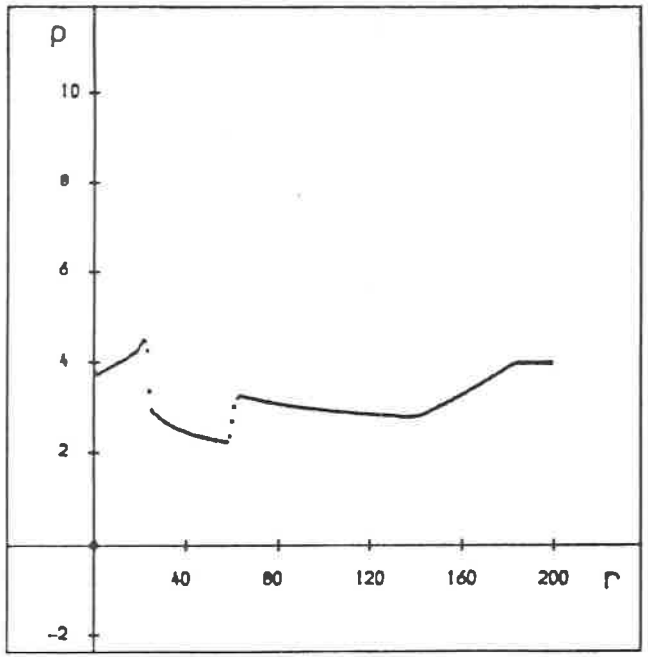

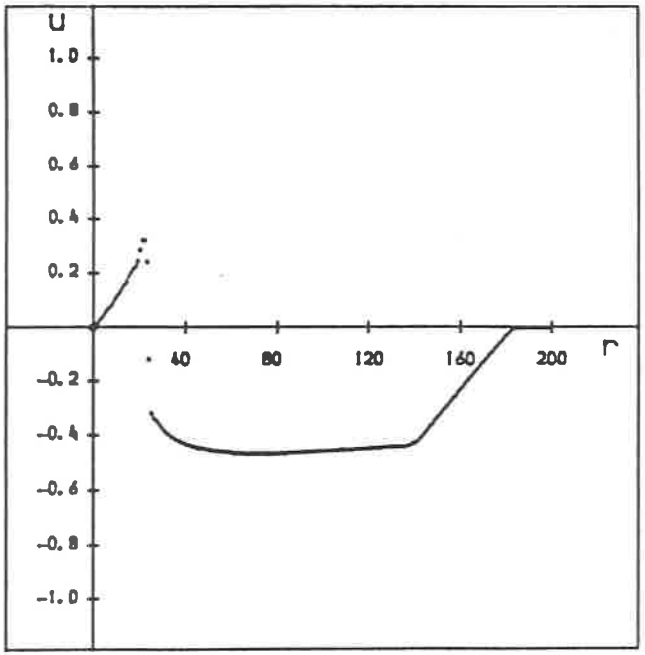

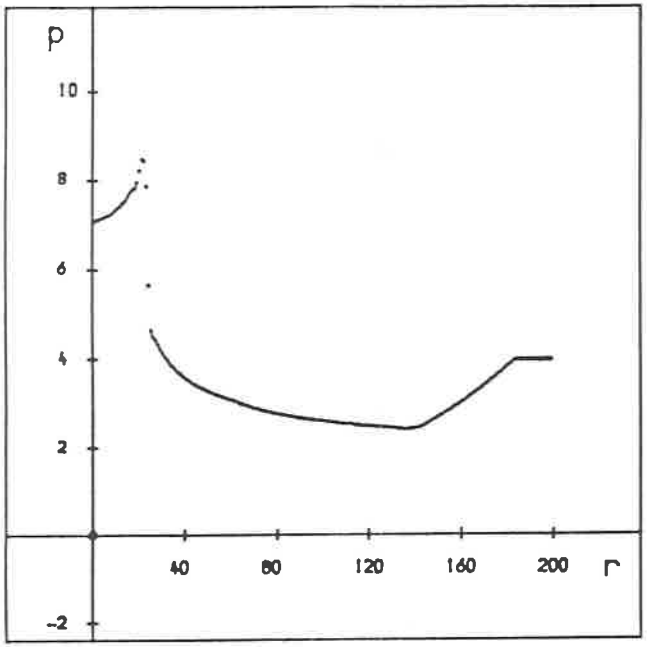

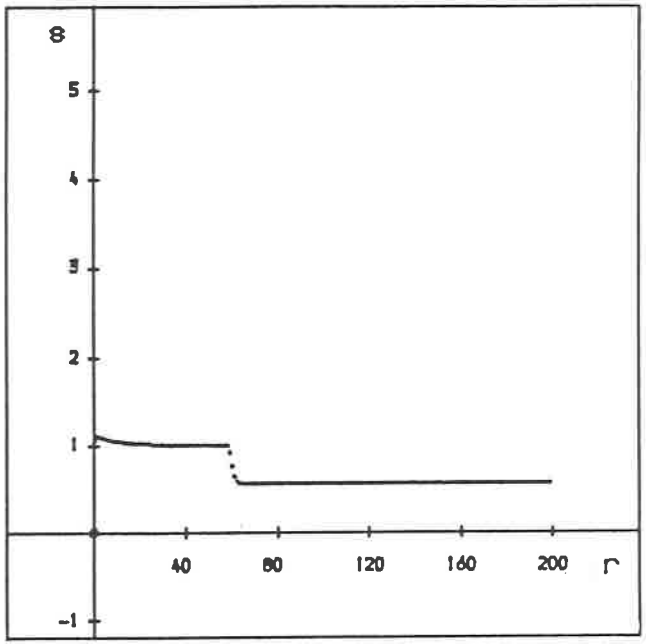

KEY

p - Density
u - Velocity
p - Pressure
s - Entropy

..... Approximate solution

PARAMETERS

$\gamma = 1.4$
200 Mesh points
280 Time steps
$\Delta r = 1$
$\Delta t = 0.25$
'Superbee' limiter used

INITIAL CONDITIONS

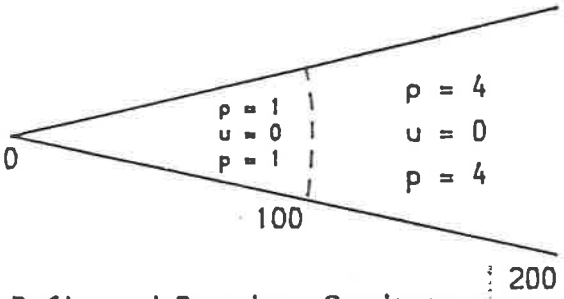

Reflected Boundary Conditions at r=0

At time t = 70 s

FIG. 10

SOLUTION OF THE EULER EQUATIONS WITH CYLINDRICAL SYMMETRY - A Converging Cylindrical Shock

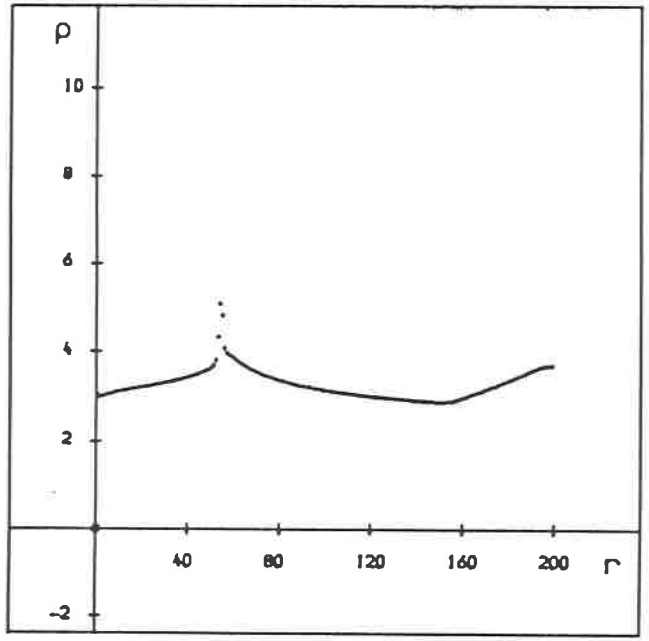

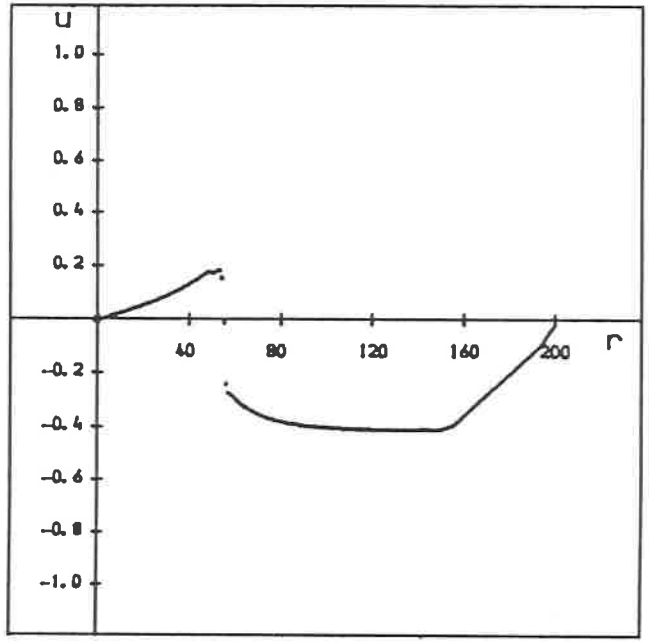

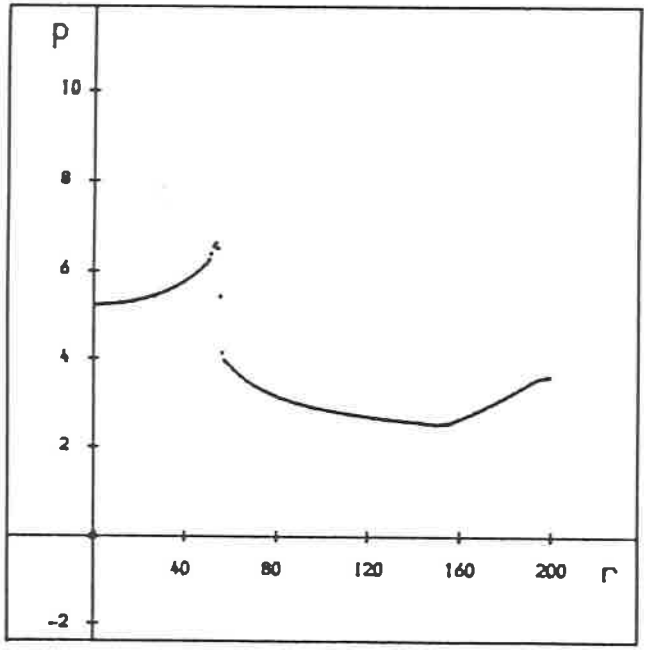

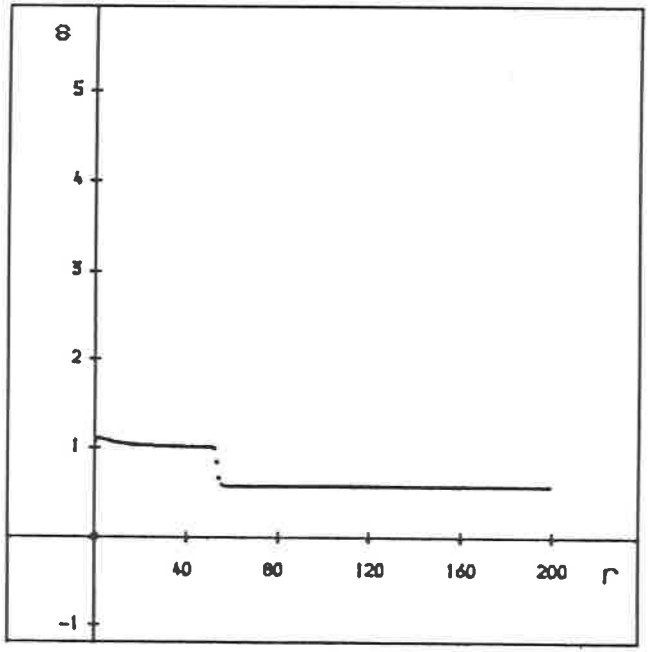

At time t = 90 s

KEY

ρ - Density
u - Velocity
p - Pressure
s - Entropy

..... Approximate solution

PARAMETERS

γ = 1.4
200 Mesh points
360 Time steps
Δr = 1
Δt = 0.25
'Superbee' limiter used

INITIAL CONDITIONS

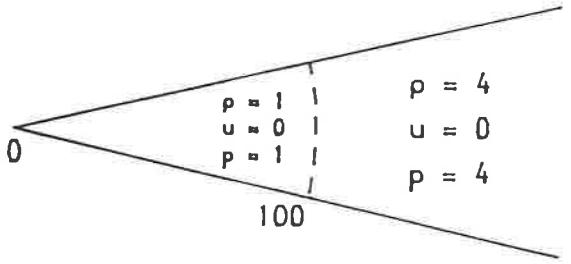

Reflected Boundary Conditions at r=0

FIG. 11

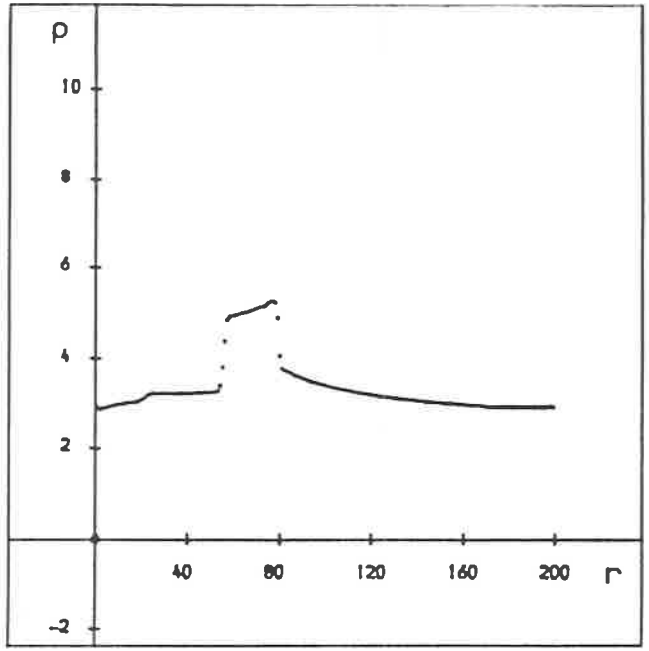

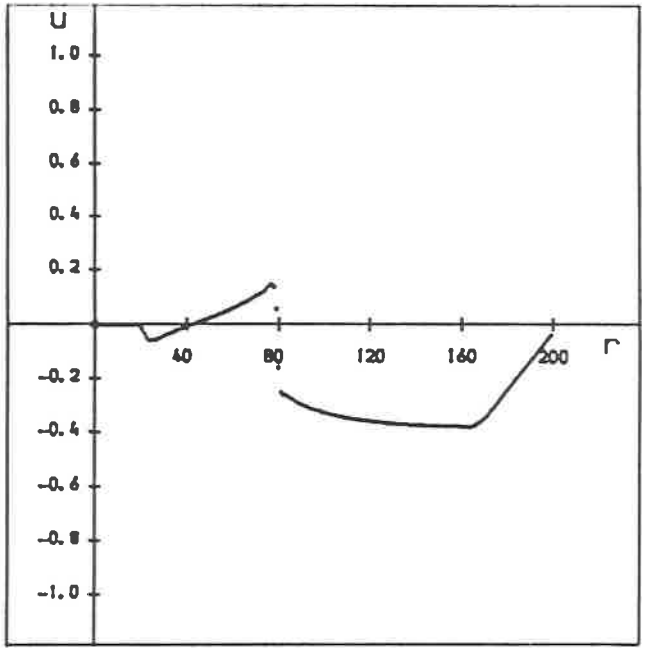

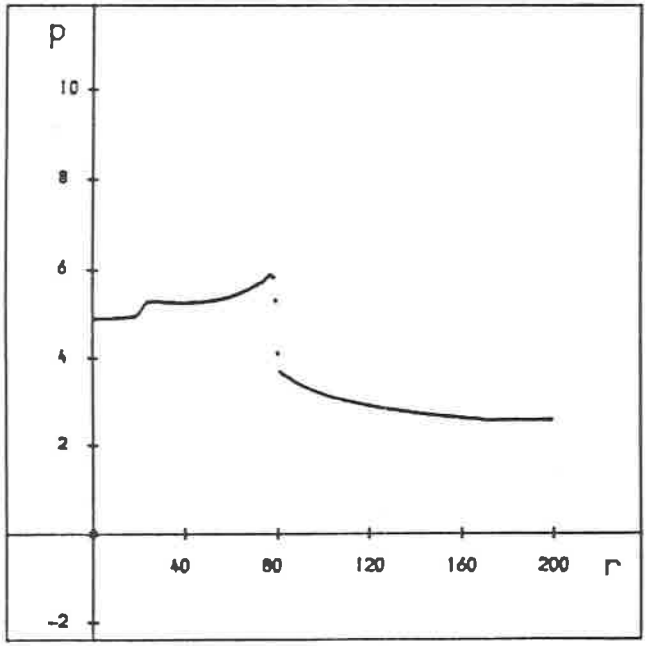

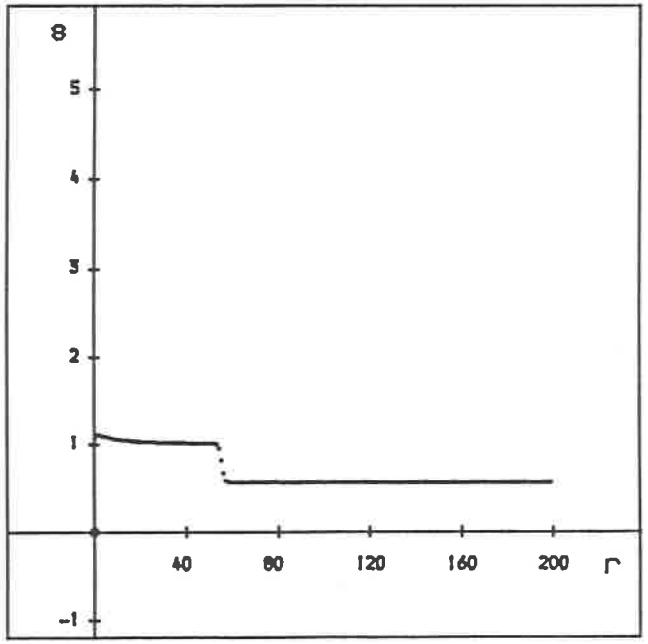

KEY

p - Density
u - Velocity
p - Pressure
s - Entropy

..... Approximate solution

PARAMETERS

$\gamma = 1.4$
200 Mesh points
440 Time steps
$\Delta r = 1$
$\Delta t = 0.25$
'Superbee' limiter used

INITIAL CONDITIONS

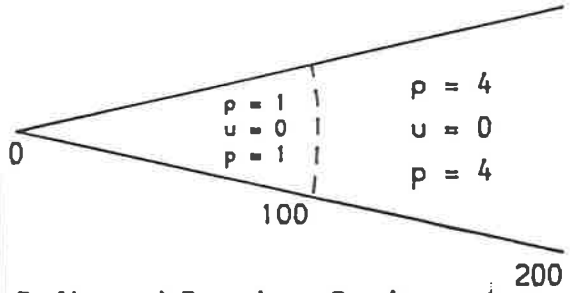

Reflected Boundary Conditions at r=0

At time t = 110 s

FIG. 12

7. CONCLUSIONS

We have extended the one-dimensional version of Roe's scheme to include cylindrically and spherically symmetric problems which give rise to source terms, and that with the approach outlined in §3 we can achieve good results on standard test problems.

We hope to extend our scheme to include variable meshes, and to study problems with axial symmetry.

ACKNOWLEDGEMENTS

I would like to express my thanks to Dr. M.J. Baines for many useful discussions and to Professor P.L. Roe for a number of invaluable suggestions.

I acknowledge the financial support of A.W.R.E., Aldermaston.

REFERENCES

1. ROE, P.L. (1981) Approximate Riemann Solvers, Parameter Vectors, and Difference Schemes. J. Comput. Phys. 27, 357.

2. ROE, P.L. (1983) Some contributions to the Modelling of Discontinuous Flows. Proc. AMS/SIAM Seminar, San Diego, to appear.

3. ROE, P.L. (1984) Efficient Construction and Utilisation of Approximate Riemann Solutions. Computing Methods in Applied Sciences and Engineering VI, ed. R. Glowinski and J.L. Lions, North Holland.

4. SWEBY, P.K. (1984) High Resolution Schemes using Flux Limiters for Hyperbolic Conservation Laws. SIAM J. Numer. Anal. 21, 995.

5. NOH, W.F. (1983) Artificial Viscosity (Q) and Artificial Heat Flux (H) errors for Spherically Divergent Shocks. UCRL preprint 89623.

6. BEN-ARTZI, M. & FALCOVITZ, J. (1983) An Upwind Second-Order Scheme for Compressible Duct Flows. Technion preprint MT 625.

7. SWEBY, P.K. (1982) A Modification of Roe's Scheme for Entropy Satisfying Solutions of Scalar Non-Linear Conservation Laws, Numerical Analysis Report, University of Reading.

8. WOODWARD, P. & COLELLA, P. (1984) The Numerical Simulation of Two-Dimensional Fluid Flow with Strong Shocks. J. Comput. Phys. 54, 115.

APPENDIX A

We include here some computations done using Roe's linearised Riemann solver together with the 'Superbee' limiter on a one-dimensional problem with slab symmetry. The problem is usually described as "Two Interacting Blast Waves".

The initial condition consists of three constant states at rest between reflecting walls. The details are given in Fig. 3.

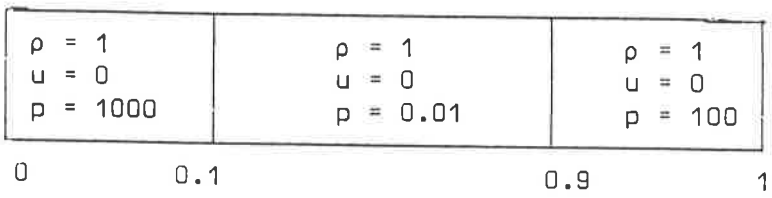

FIG. 3

Two strong blast waves develop and collide producing a complex flow. A detailed description of the time evolution can be found in [8].

We use the Superbee limiter and 400 mesh points. The results show the essential features of the flow as described in [8] and compare well.

SOLUTION OF THE EULER EQUATIONS WITH SLAB SYMMETRY - Two Interacting Blast Waves

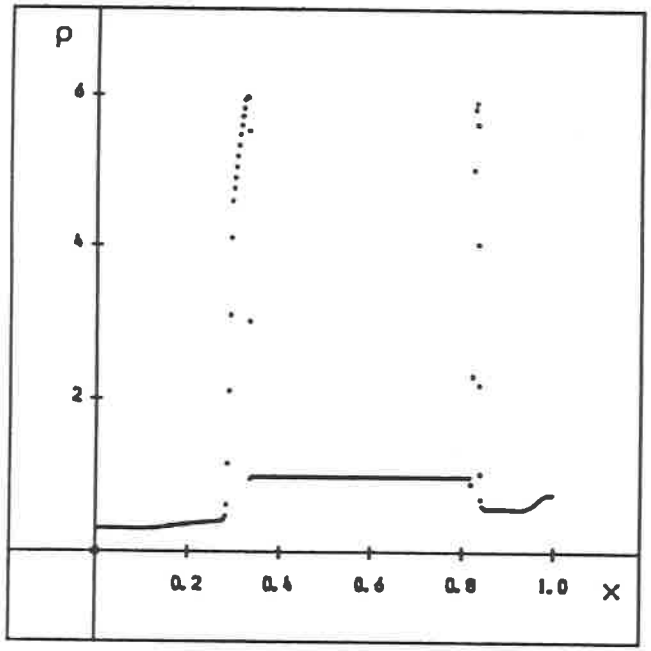

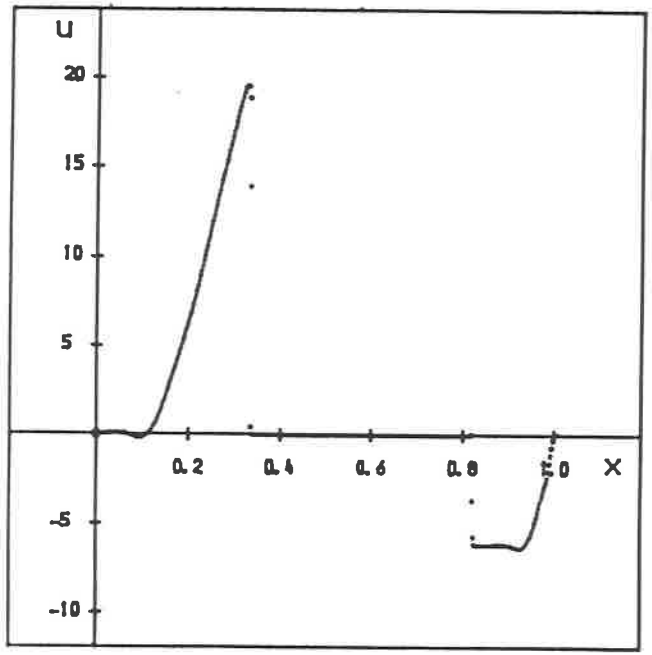

At time t = 0.01 s

KEY

ρ - Density
u - Velocity

..... Approximate solution

PARAMETERS

$\gamma = 1.4$
400 Mesh points
250 Time steps
$\Delta x = 0.0025$
$\Delta t = 0.00004$
'Superbee' limiter used

INITIAL CONDITIONS

ρ = 1	ρ = 1	ρ = 1
u = 0	u = 0	u = 0
p=1000	p=0.01	p=100

0 0.1 0.9 1

Reflected Boundary Conditions
at x = 0 and x = 1

SOLUTION OF THE EULER EQUATIONS WITH SLAB SYMMETRY - Two Interacting Blast Waves

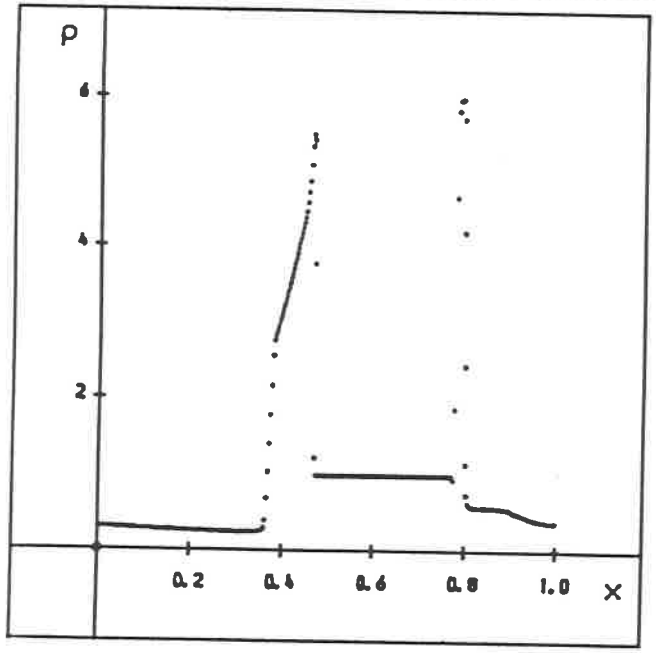

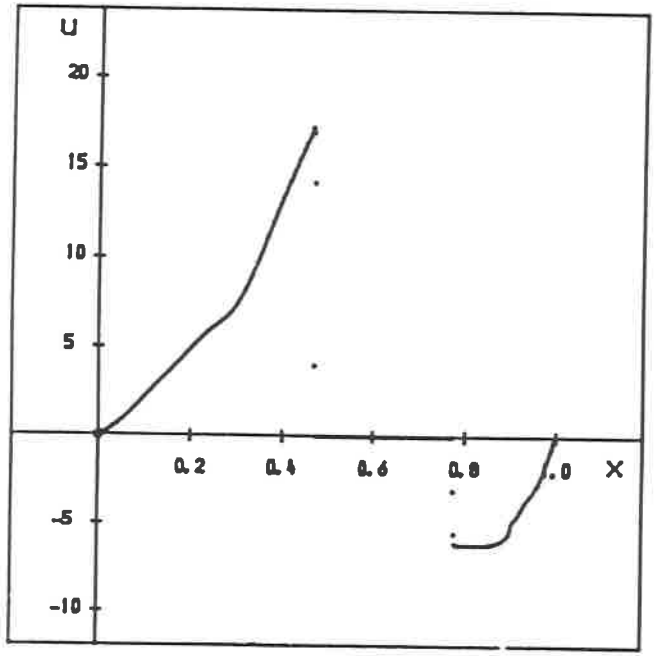

At time t = 0.016 s

KEY

ρ - Density
u - Velocity

..... Approximate solution

PARAMETERS

γ = 1.4
400 Mesh points
400 Time steps
Δx = 0.0025
Δt = 0.00004
'Superbee' limiter used

INITIAL CONDITIONS

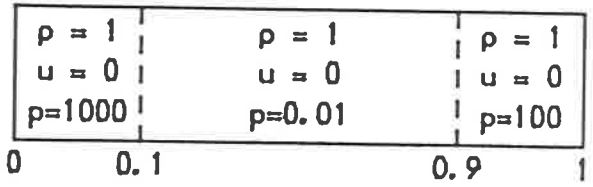

Reflected Boundary Conditions
at x = 0 and x = 1

SOLUTION OF THE EULER EQUATIONS WITH SLAB SYMMETRY - Two Interacting Blast Waves

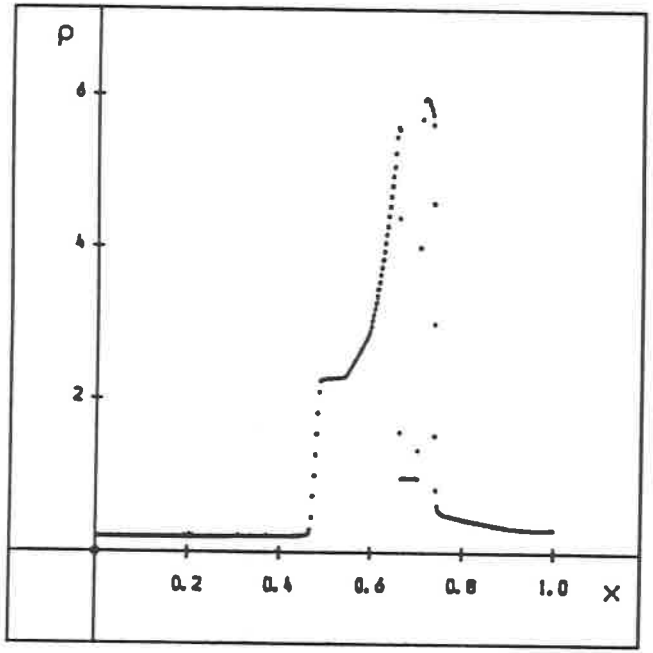

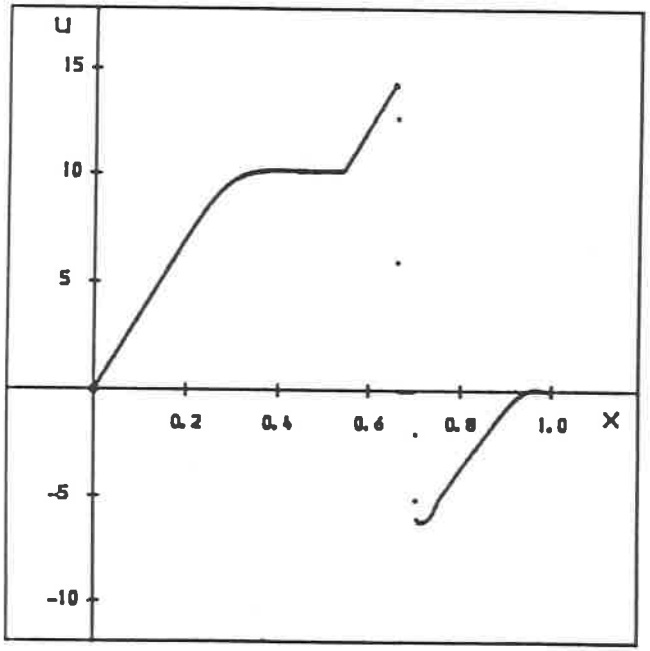

At time t = 0.026 s

KEY

ρ - Density
u - Velocity

..... Approximate solution

PARAMETERS

γ = 1.4
400 Mesh points
650 Time steps
Δx = 0.0025
Δt = 0.00004
'Superbee' limiter used

INITIAL CONDITIONS

ρ = 1	ρ = 1	ρ = 1
u = 0	u = 0	u = 0
p=1000	p=0.01	p=100

0 0.1 0.9 1

Reflected Boundary Conditions
at x = 0 and x = 1

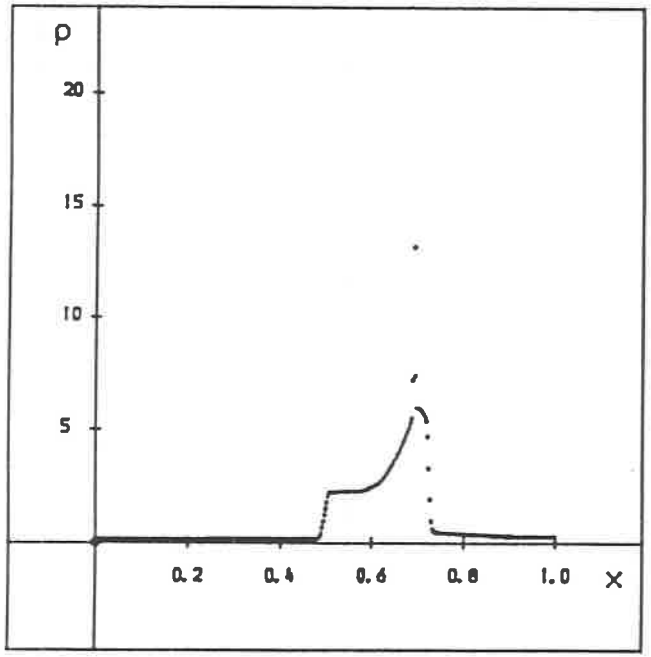

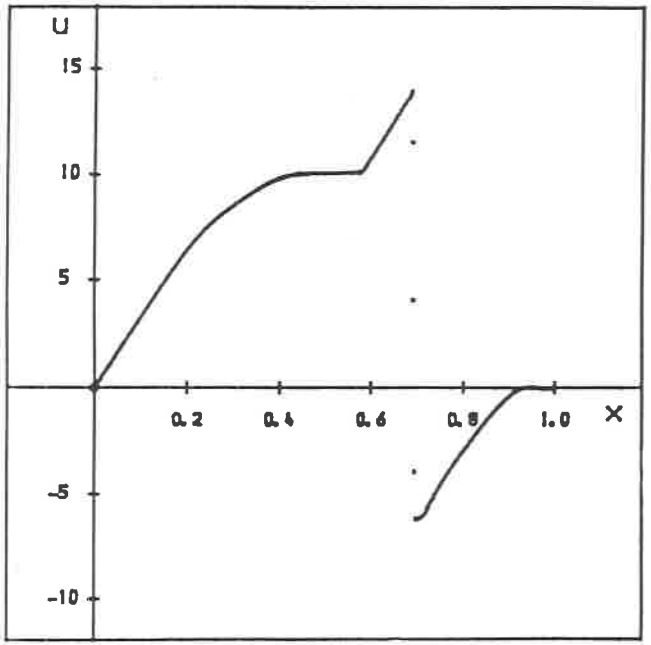

At time t = 0.028 s

KEY

ρ - Density
u - Velocity

..... Approximate solution

PARAMETERS

γ = 1.4
400 Mesh points
700 Time steps
Δx = 0.0025
Δt = 0.00004
'Superbee' limiter used

INITIAL CONDITIONS

ρ = 1 u = 0 p=1000	ρ = 1 u = 0 p=0.01	ρ = 1 u = 0 p=100

0 0.1 0.9 1

Reflected Boundary Conditions
at x = 0 and x = 1

SOLUTION OF THE EULER EQUATIONS WITH SLAB SYMMETRY - Two Interacting Blast Waves

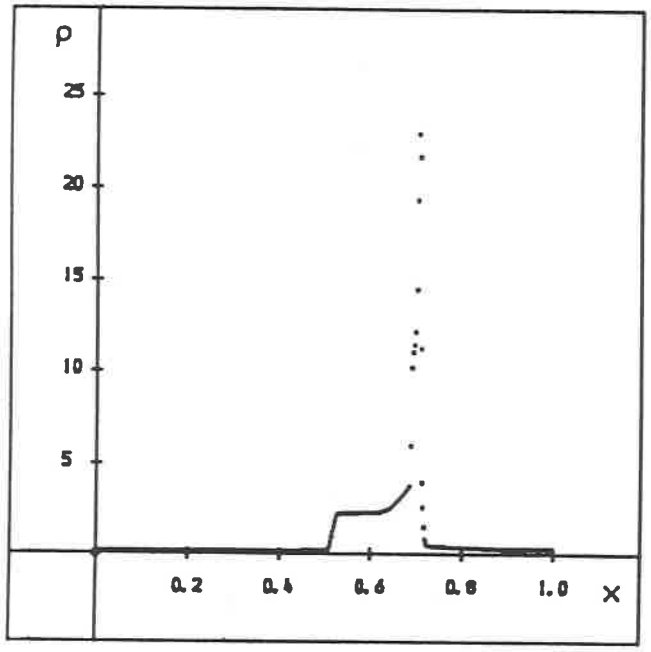

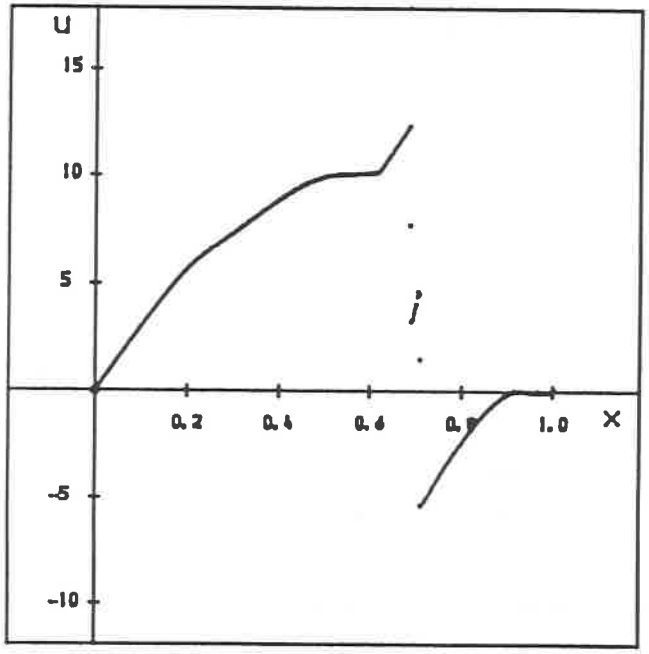

At time t = 0.03 s

KEY

ρ - Density
u - Velocity

..... Approximate solution

PARAMETERS

$\gamma = 1.4$
400 Mesh points
750 Time steps
$\Delta x = 0.0025$
$\Delta t = 0.00004$
'Superbee' limiter used

INITIAL CONDITIONS

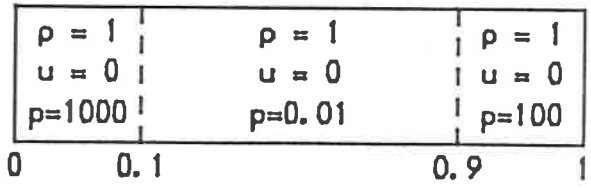

Reflected Boundary Conditions
at x = 0 and x = 1

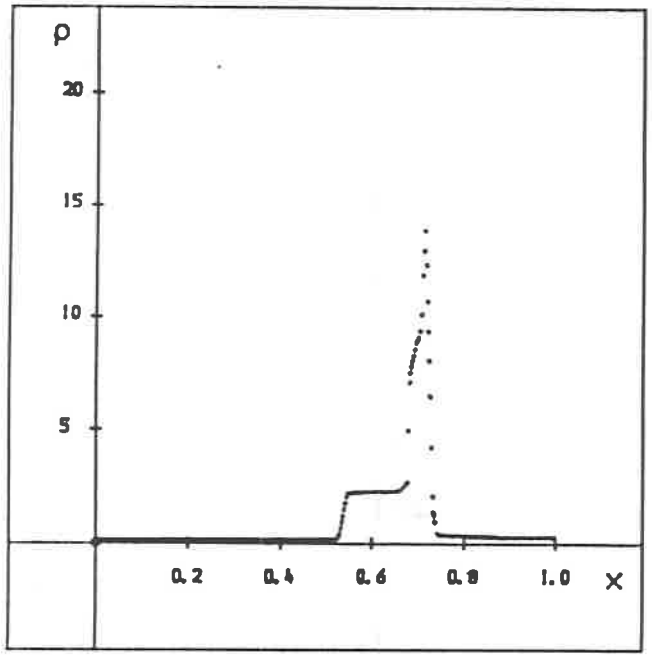

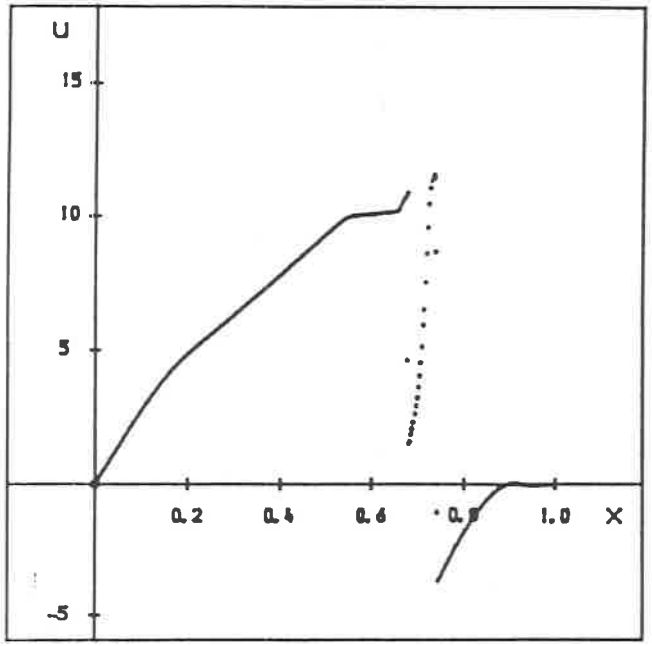

At time t = 0.032 s

KEY

ρ - Density
u - Velocity

..... Approximate solution

PARAMETERS

γ = 1.4
400 Mesh points
800 Time steps
Δx = 0.0025
Δt = 0.00004
'Superbee' limiter used

INITIAL CONDITIONS

ρ = 1 u = 0 p=1000	ρ = 1 u = 0 p=0.01	ρ = 1 u = 0 p=100

0 0.1 0.9 1

Reflected Boundary Conditions
at x = 0 and x = 1

SOLUTION OF THE EULER EQUATIONS WITH SLAB SYMMETRY - Two Interacting Blast Waves

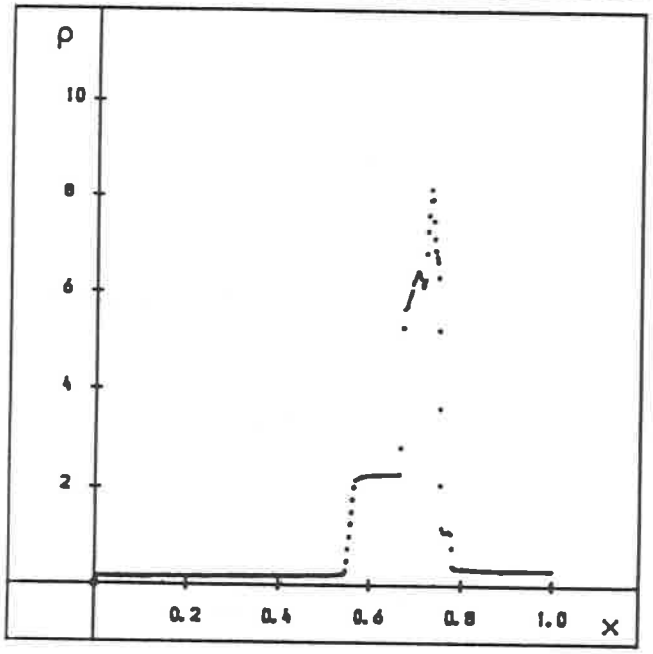

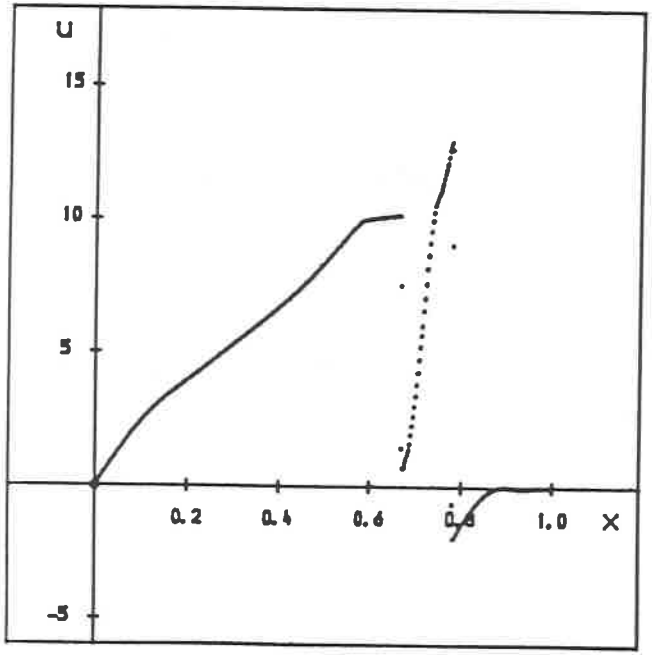

At time t = 0.034 s

KEY

ρ - Density
u - Velocity

..... Approximate solution

PARAMETERS

γ = 1.4
400 Mesh points
850 Time steps
Δx = 0.0025
Δt = 0.00004
'Superbee' limiter used

INITIAL CONDITIONS

ρ = 1 u = 0 p=1000	ρ = 1 u = 0 p=0.01	ρ = 1 u = 0 p=100

0 0.1 0.9 1

Reflected Boundary Conditions
at x = 0 and x = 1

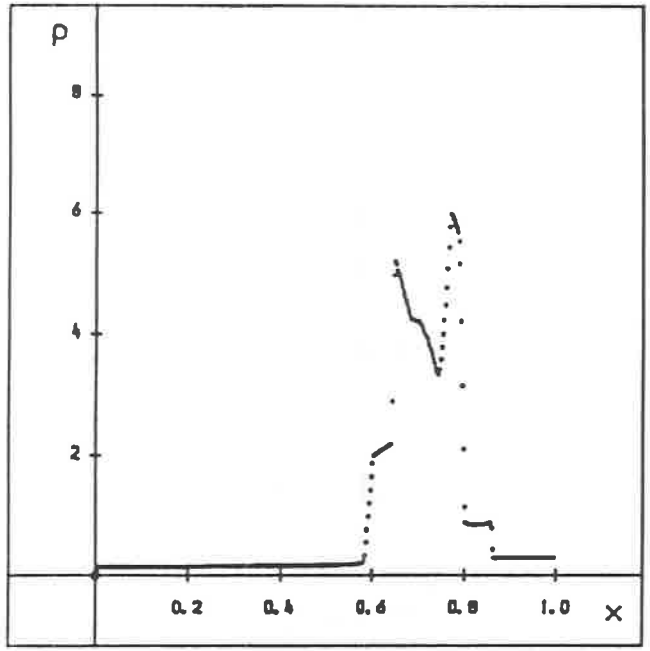

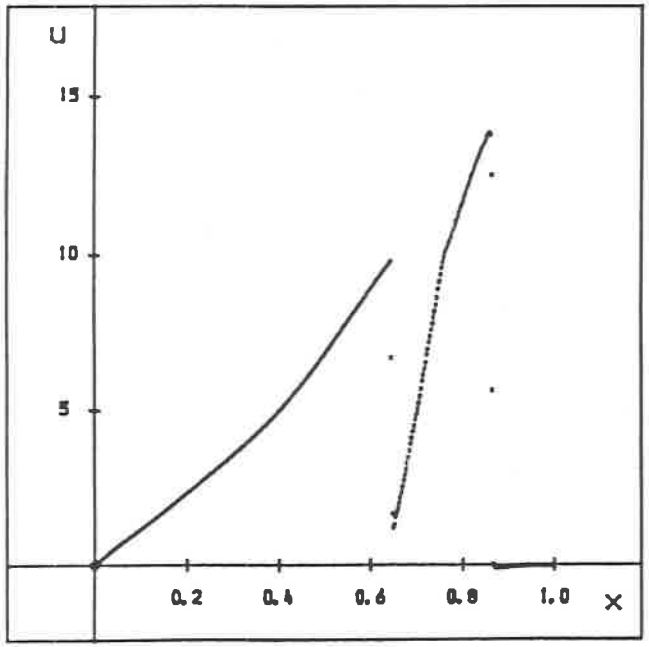

At time t = 0.038 s

KEY

ρ - Density
u - Velocity

..... Approximate solution

PARAMETERS

$\gamma = 1.4$
400 Mesh points
950 Time steps
$\Delta x = 0.0025$
$\Delta t = 0.00004$
'Superbee' limiter used

INITIAL CONDITIONS

ρ = 1	ρ = 1	ρ = 1
u = 0	u = 0	u = 0
p=1000	p=0.01	p=100

0 0.1 0.9 1

Reflected Boundary Conditions
at x = 0 and x = 1

APPENDIX B

Consider a general orthogonal curvilinear co-ordinate system (x_1,x_2,x_3) where a line element $\underline{ds}$ is given by

$$\underline{ds} = h_1 dx_1 \hat{\underline{x}}_1 + h_2 dx_2 \hat{\underline{x}}_2 + h_3 dx_3 \hat{\underline{x}}_3$$

and $\hat{\underline{x}}_1$, $\hat{\underline{x}}_2$, $\hat{\underline{x}}_3$ are orthogonal. The vector $\hat{\underline{x}}_i$ is of unit length and parallel to the co-ordinate lines with x_i increasing. Consider also a scalar field $\alpha = \alpha(x_1,x_2,x_3)$ a vector field $\underline{b} = \underline{b}(x_1,x_2,x_3) = b_1 \hat{\underline{x}}_1 + b_2\hat{\underline{x}}_2 + b_3\hat{\underline{x}}_3$, and a 3×3 tensor $\underline{\underline{B}} = (B_{ij})$. Then the definitions of grad α, div $\underline{b}$ and div $\underline{\underline{B}}$ are as follows

$$\text{grad } \alpha = \frac{1}{h_1} \frac{\partial \alpha}{\partial x_1} \hat{\underline{x}}_1 + \frac{1}{h_2} \frac{\partial \alpha}{\partial x_2} \hat{\underline{x}}_2 + \frac{1}{h_3} \frac{\partial \alpha}{\partial x_3} \hat{\underline{x}}_3$$

$$\text{div } \underline{b} = \frac{1}{h_1 h_2 h_3} \left(\frac{\partial}{\partial x_1} (h_2 h_3 b_1) + \frac{\partial}{\partial x_2} (h_1 h_3 b_2) + \frac{\partial}{\partial x_3} (h_1 h_2 b_3) \right)$$

and

$$(\text{div } \underline{\underline{B}})_i = \frac{1}{h_1 h_2 h_3} \left[\frac{\partial}{\partial x_1} (h_2 h_3 B_{1i}) + \frac{\partial}{\partial x_2} (h_1 h_3 B_{2i}) + \frac{\partial}{\partial x_3} (h_1 h_2 B_{3i}) \right.$$

$$\left. + \frac{B_{ij}}{h_i h_j} \frac{\partial h_i}{\partial x_j} + \frac{B_{ki}}{h_i h_k} \frac{\partial h_i}{\partial x_k} - \frac{B_{jj}}{h_i h_j} \frac{\partial h_j}{\partial x_i} - \frac{B_{kk}}{h_i h_k} \frac{\partial h_k}{\partial x_i} \right]$$

where (ijk) is a cyclic permutation of (123).

If we now write $\underline{\underline{D}} = \alpha \underline{\underline{B}}$, then $(\text{div } \underline{\underline{D}})_i = (\text{div}(\alpha \underline{\underline{B}}))_i =$

$$\frac{1}{h_1 h_2 h_3} \left[\frac{\partial}{\partial x_1} (h_2 h_3 \alpha B_{1i}) + \frac{\partial}{\partial x_2} (h_1 h_3 \alpha B_{2i}) + \frac{\partial}{\partial x_3} (h_1 h_2 \alpha B_{3i}) \right]$$

$$+ \frac{\alpha B_{ij}}{h_i h_j} \frac{\partial h_i}{\partial x_j} + \frac{\alpha B_{ki}}{h_i h_h} \frac{\partial h_i}{\partial x_k} - \frac{\alpha B_{jj}}{h_i h_j} \frac{\partial h_j}{\partial x_i} - \frac{\alpha B_{kh}}{h_i h_k} \frac{\partial h_k}{\partial x_i}$$

and by carrying out the differentiation we get

$$(\text{div } \underline{\underline{D}})_i = \alpha(\text{div } \underline{\underline{B}})_i + \frac{B_{1i}}{h_1}\frac{\partial \alpha}{\partial x_1} + \frac{B_{2i}}{h_2}\frac{\partial \alpha}{\partial x_2} + \frac{B_{3i}}{h_3}\frac{\partial \alpha}{\partial x_3}$$

$$= (\alpha \text{ div } \underline{\underline{B}}) + (\text{grad } \alpha)\cdot \begin{pmatrix} B_{1i} \\ B_{2i} \\ B_{3i} \end{pmatrix}$$

Thus $\text{div } \underline{\underline{D}} = \text{div}(\alpha \underline{\underline{B}}) = \alpha \text{ div } \underline{\underline{B}} + (\text{grad } \alpha)\cdot\underline{\underline{B}}$. In particular, if $\underline{\underline{B}} = \underline{\underline{I}}$, the 3x3 identity matrix, then $(\text{div } \underline{\underline{I}})_i = \frac{1}{h_i h_j h_k}\frac{\partial}{\partial x_i}(h_j h_k) - \frac{1}{h_i h_j}\frac{\partial h_j}{\partial x_i} - \frac{1}{h_i h_k}\frac{\partial}{\partial}$

so

$$\text{div } (\alpha\underline{\underline{I}}) = \alpha \text{ div } \underline{\underline{I}} + (\text{grad } \alpha)\cdot\underline{\underline{I}}$$

$$= (\text{grad } \alpha)\cdot\underline{\underline{I}} = \text{grad } \alpha \ .$$

If we specialise to cartesian, cylindrical or spherical geometries we have

(i) Cartesian $x_1 = x$, $x_2 = y$, $x_3 = z$, $h_1 = 1$, $h_2 = 1$, $h_3 = 1$.

So grad $\alpha = (\partial\alpha/\partial x_i, \ \partial\alpha/\partial x_2, \ \partial\alpha/\partial x_3)$

and $\text{div } \underline{b} = \frac{\partial b_1}{\partial x_1} + \frac{\partial b_2}{\partial x_2} + \frac{\partial b_3}{\partial x_3}$.

(ii) Cylindrical $x_1 = R$, $x_2 = \phi$, $x_3 = z$, $h_1 = 1$, $h_2 = R$, $h_3 = 1$.

So grad $\alpha = \left(\frac{\partial\alpha}{\partial R}, \ \frac{1}{R}\frac{\partial\alpha}{\partial\phi}, \frac{\partial\alpha}{\partial z}\right)$

and $\text{div } \underline{b} = \frac{1}{R}\frac{\partial}{\partial R}(Rb_1) + \frac{1}{R}\frac{\partial b_2}{\partial\phi} + \frac{\partial b_3}{\partial z}$.

(iii) Spherical $x_1 = r$, $x_2 = \theta$, $x_3 = \phi$, $h_1 = 1$, $h_2 = r$, $h_3 = r\sin\theta$

So grad $\alpha = \left(\frac{\partial\alpha}{\partial r}, \ \frac{1}{r}\frac{\partial\alpha}{\partial\theta}, \ \frac{1}{r\sin\theta}\frac{\partial\alpha}{\partial\phi}\right)$

and $\operatorname{div} \underline{b} = \frac{1}{r^2} \frac{\partial}{\partial r} (r^2 b_1) + \frac{1}{r \sin\theta} \frac{\partial}{\partial \theta} (\sin\theta b_2) + \frac{1}{r \sin\theta} \frac{\partial b_3}{\partial \phi}$.

If we assume symmetry so that $\alpha = \alpha(x_1)$ $\underline{b} = \underline{b}(x_1)$, then div and grad are only the same in case (i).